 doi:10.20944/preprints202207.0378.v1

Article

Metabolomic Aspects of Conservative and Resistance-related Elements of Response to *Fusarium culmorum* in the Grass Family

Anna Piasecka[1,*,†], Aneta Sawikowska [1,2,†], Natalia Witaszak[3], Agnieszka Waśkiewicz[4], Marta Kańczurzewska[5], Joanna Kaczmarek[3] and Justyna Lalak-Kańczugowska[1]

[1]Institute of Bioorganic Chemistry of the Polish Academy of Sciences, Poznań, Poland, apiasecka@ibch.poznan.pl; asawikowska@ibch.poznan.pl; jlalak@ibch.poznan.pl
[2]Department of Mathematical and Statistical Methods, Poznań University of Life Sciences, Poznań, Poland; aneta.sawikowska@up.poznan.pl
[3] Institute of Plant Genetic of the Polish Academy of Sciences, Poznań, Poland, nwit@igr.poznan.pl; jkac@igr.poznan.pl
[4] Faculty of Forestry and Wood Technology, Poznan University of Life Sciences, Poznań, Poland; agnieszka.waskiewicz@up.poznan.pl
[5] Faculty of Control, Robotics and Electrical Engineering, Institute of Mathematics, Poznan University of Technology, Poznań, Poland, marta.kanczurzewska@put.poznan.pl
[†]These authors. are equal first authors of the manuscript
*Corresponding author: apiasecka@ibch.poznan.pl

Abstract: Background: *Fusarium head blight (FHB) is a serious fungal disease of crop plants due to* substantial yield reduction and production of mycotoxins in the infected grains. The breeding progress in increasing resistance with maintaining a high yield is not possible without a thorough examination of the molecular basis of plant immunity responses; **Methods**: LC-MS based metabolomics approaches powered by three-way ANOVA and differentially accumulated metabolites (DAMs) selection, correlation network and functional enrichment were conducted on grains of resistant and susceptible to FHB genotypes of barley and wheat as well as model grass *Brachypodium distachyon* (Bd) still poorly known at metabolomic level; **Results**: We selected common and genotype-specific DAMs in response to *F. culmorum* inoculation. Immunological reaction at metabolomic level was strongly diversified between resistant and susceptible genotypes. DAMs common for all tested species from porphyrins, flavonoids and phenylpropanoids metabolic pathways were highly correlated and reflects conservativeness in FHB response in Poaceae family. Resistant related DAMs belonged to different structural classes including tryptophan derived metabolites, pirimidines, amino acids proline and serine as well as phenylpropanoids and flavonoids. Physiological response to *F. culmorum* of Bd was close to barley and wheat genotypes however, metabolomic changes were strongly diversified. **Conclusions**: Combined targeted and untargeted metabolomics provides comprehensive knowledge about significant elements of plant immunity with potential of being molecular biomarkers of enhance resistance to FHB in grass family. Thorough examination of Bd21 metabolome in juxtaposition with barley and wheat diversified genotypes facilitate their setting as model grass for plant-microbe interaction.

Keywords: FHB; plant metabolomic; plant-pathogen interaction; barley; wheat; *Brachypodium distachyon*; pathway enrichment

1. Introduction

Cereal crops in Europe is dominated by common wheat (44% of yield), as well as the steadily growing part by barley (18,6%), clearly ahead grain maize (23,4%) (Eurostat, https://ec.europa.eu/eurostat). Nevertheless, the resulting cereals yield reaches approximately half of the genetic potential, and one of the main reason for yield reduction are diseases caused by pathogenic fungi, in particular from toxinogenic genus *Fusarium*

Preprints (www.preprints.org) | NOT PEER-REVIEWED | Posted: 26 July 2022 doi:10.20944/preprints202207.0378.v1

[1]. The most common symptoms of Fusarium wilt in cereal are for instant Fusarium head blight (FHB), root rot, and Fusarium seedling blight (FSB). *Fusarium head blight* caused by number of pathogenic *Fusarium* species including F*usarium culmorum,* is a serious fungal pathogen of small cereal grains like wheat, barley, oats as well as forage grasses [2]. The disease develops from infection at anthesis and spreads until grain harvest resulting in handicap of kernels development. The main problems from the FHB is grain contamination with mycotoxins, such as zearalenone (ZEN), fusarins and type B trichothecenes among which deoxynivalenol (DON) which is considered to be the most toxic compound produced by *F. culmorum* [3]. There are no cereals varieties fully immune to FHB as it is a quantitative trait, therefore the efficient crop breeding must be strongly supported by comprehensive knowledge regarding the molecular mechanisms of pathogenesis and plant-fungus interactions. One of the basic factors influencing the resistance of cereals is the composition of low molecular metabolites and the speed of their activation and biosynthesis.

In spite of many immunological similarities among genetically close species of Poaceae family there is high diversification in metabolite profiles in that taxonomic group. Examples are benzoxazinoids detected in wheat, rye and maize whereas barley and Bd have lost of Bx biosynthetic genes [4]. Cereals response to FHB in context of conserved mechanism should be therefore examined in complex setting of cultivars distinct in FHB resistance. Various defensive metabolites are derived via the phenylpropanoid/shikimic acid pathway in Poaceae plants. Accumulation of hydroxycinnamic acid amides and phenolic acids glycosides in wheat response to FHB was correlated to cell wall thickening and inhibition of pathogen growth [3]. The key enzymes of phenylpropanoid biosynthesis such as cinnamyl alcohol dehydrogenase, caffeoyl-CoA O-methyltransferase, caffeic acid *O*-methyltransferase, flavonoid *O*-methyltransferase, agmatine coumaroyltransferase and peroxidase were up-regulated in response to *F. graminearum* and DON production [5]. A number of metabolomics studies have investigated flavonoids that were correlated to FHB resistance in barley [6,7] and wheat [8]. Among them glycosidic form of flavonols kaempferol and quercetin are observed as highly abundant group which can inhibit fungal transcription [9]. A deficiency of proanthocyanidin production facilitated an increased penetration of the barley seed testa layer by both *F. graminearum* and *F. culmorum* [10].

Recently, much attention is paid to antifungal properties of polyamines. Putrescine, spermidine and spermine were noted as rapidly induced in FHB and contributed to induction of DON biosynthesis by *F. graminearum* [11]. Polyamines acylated with hydroxycinnamic acids are accumulating during pathogenesis in barley [6,7], wheat [11] and model cereal plant *Brachypodium distachyon* [5].

Brachypodium distachyon (Bd) is used as a model system for functional genomics of grasses. In recent years Bd emerges as model plant for studies of cereal crops-pathogen interactions [12]. To date, however, there has been very little evidence to demonstrate conservation of function between *B. distachyon* and cereals with respect to immunological processes at the molecular level. Many biological tests and histopathological studies showed that *Fusarium* sp. infect Bd in a similar manner as wheat [12] but also positive correlation was shown between Bd and barley physiology. To enhance the knowledge of Bd as model grass we compare the most used Bd 21 line still poorly known at metabolomic level to well characterized genotypes of wheat and barley with widely differing susceptibility to FHB symptoms. Therefore, we presented conservative and genotype-specific metabolites in relation to biosynthetic pathways in term of susceptibility and resistance to FHB in expanded context of Poaceae family. Distinction between conservative and resistant-related defense elements can also facilitate strategies for plant breeding in cereal crops with enhance resistance to FHB.

Preprints (www.preprints.org) | NOT PEER-REVIEWED | Posted: 26 July 2022 doi:10.20944/preprints202207.0378.v1

2. Materials and Methods

2.1. Reagents and chemicals

Acetonitrile for LC-MS analyses was from VWR Chemicals (USA), formic acid was from Merck Life Science (Germany). Ultrapure water was obtained from a Millipore Direct Q3 device. Standards of compounds (caffeic acid, isoorientin, apigenin 6-C-glucoside-8-C-arabinoside, luteolin-3,7-di-O-glucoside, tricin 7-O-glucoside, tricin glucosylrhamnoside) were purchased from the Extrasynthese (Genay, France). Isoorientin 2''-O-glucoside, isovitexin 7-O-glucoside, isoscoparin 2''-O-glucoside and apigenin 6-C-arabinoside-8-C-glucoside were purified from plant material and their structures were confirmed with NMR analysis as described previously [13]. Standard of zearalenone, tryptophan, 2,2-diphenyl-1-picrylhydrazyl and ascorbic acid were from Merck Life Science. Hypochloride was from BioShop.

2.2. Plant growth and inoculation

Two spring wheat (*Triticum aestivum*) and barley (*Hordeum vulgare*) genotypes differing in their susceptibility to *F. culmorum* and in addition to model plant *Brachypodium distachyon* line Bd21 (Bd21) were selected for experiments. For simplicity, genotypes with high susceptibility to FHB will be further described as susceptible while genotype with reduced susceptibility to FHB will be described as resistant, although in fact it is not complete resistance.

Plants were cultivated in the phytotron of the Plant Cultivation Center of Institute of Plant Genetics Polish Academy of Sciences, Poland, Poznan. Barley genotypes came from recombinant inbred lines of *Hordeum vulgare* MCam obtained from the cross between the Polish cultivar Lubuski and a Syrian breeding line—Cam/B1/CI08887//CI05761, selected from the own materials of the Institute of Plant Genetics of the Polish Academy of Sciences on the basis of previous studies [14]. Two extremely different lines of barley MCam 88 line (hereafter signed as Hs) and resistant MCam 59 line (hereafter signed as Hr) were taken for metabolomic analysis. The sensitive cultivar Radocha [15] (hereafter signed as Ts) and highly resistant line CJ 9306 [16] (hereafter signed as Tr) of wheat were from Breeding Company Strzelce, Poland. Bd21 line was provided by the National Plant Germplasm System of USDA-ARS.

Seeds were surface-sterilized by soaking in 2.5% sodium hypochlorite for 30 min then washed thoroughly in sterile deionized water. The seeds were sown into Ø 30 cm pots filled with soil in growth chambers. During first month plants were grown at short-day conditions (10 h light, 14 h dark) at 16˚C and then switched to long-day conditions (16 h light, 8 h dark) at temperature 21 ˚C at light/14 ˚C at dark with humidity 60% of RH for acceleration of flowering. Plants were grown in two principal experiments.

An inoculation was performed with the fungus *Fusarium culmorum* KF846 from the Institute of Plant Genetic, Polish Academy of Sciences, Poland, Poznan collection. To better characterized of *F. culmorum* strain the gene expression of key biosynthetic genes (ZEA synthase – *ZEA2*, Zinc finger transcription factor - *TRI6*, Trichodiene synthase - *TRI5*) were performed leading to characterization of mycotoxinogenic profile of this strain (supplementary method 1). In order to prepare the spore suspension, spores were washed from the surface of a 2-week-old colony growing on PDA medium (Potato, Dextrose, Agar, Oxoid). The inoculation was carried out at the concentration of 2 ×106 spores / ml.

The inoculation with fungal spores was carried out in the milk stage of the spikes (at 61 stage of BBCH scale) by spraying. For barley and wheat it was approx. 8 weeks and for Bd21, 12 weeks from sowing. After inoculation for 24 hours, the plants were kept in the dark upon mist irrigation for increasing infection efficiency. For gene expression analysis, samples (spikes) were collected 24 and 48 h after inoculation. For metabolomic analysis, samples were collected at 4 and 6 days after inoculation. For antioxidant and mycotoxin analysis samples were collected at 6 days after inoculation. All collected samples were immediately frozen in liquid nitrogen and stored in -80 ˚C until assay.

Preprints (www.preprints.org) | NOT PEER-REVIEWED | Posted: 26 July 2022 doi:10.20944/preprints202207.0378.v1

2.3. Quantification of Fusarium culmorum

DNA was extracted using the CTAB (cetyltrimethyl ammonium bromide). The samples were suspended in 650 µl CTAB and incubated at 65°C for 20 min. The volume of 500 µL CHCl3 was added and centrifuged at 12 879 g for 15 min. DNA was precipitated with 65 µl 3M sodium acetate, pH 5.4, and two volumes of ice cold 99.8% ethanol. The tubes were stored at −20°C overnight and centrifuged at 17 530 × g for 5 min. The pellets were washed with 70% ethanol, centrifuged at 17 530 × g for 5 min and fully dissolved in 100 µl of TE buffer.

The real-time PCR was performed in 10 µl containing 7.5 µl AmpliQ Real-Time PCR Opti Probe Kit (Novazym, Poznań, Poland), 100 nM of FAM-labeled probe and 300 nM of forward and reverse *F. culmorum* primers [17]. Thermal cycling parameters for a quantitative fungal DNA detection were: 95°C for 2 min followed by 40 cycles of 95°C for 15 s and 60°C for 30 s. Nuclease-free water was used as the no-template control. A standard curve was generated by plotting the Ct value for each sample of standard series of the amount of fungal biomass (10–0.001 mg/g). All the samples were tested in triplicate.

2.4. Zearalenone measurement

Organic solvents (HPLC grade) for analysis was purchase from Sigma–Aldrich (Steinheim, Germany). The HPLC - grade water was obtained by using a Milli-Q system (Millipore, Bedford, USA). The stock solution of zearalenonee (ZEN) was dissolved in methanol (1 mg/mL) and stored at -20°C. ZEN was extracted and purified on a ZearalaTest column (Vicam, Milford, CT, USA) according to a procedure described previously [18]. The chromatographic elution of ZEN was done on Waters 2695 HPLC (Waters, Milford, CT, USA) with Waters 2996 Photodiode Array Detector – and a Nova Pak C-18 column (150 × 3.9 mm). Data were processed using the Empower software (Waters, Milford, CT, USA). Quantitative estimation of ZEN was performed by measuring the peak areas at the retention time according to the relative calibration curve. The limit of detection was 0.01 µg m/L.

2.5. Antioxidative activity measurement

Antioxidative state was measured by 2,2-diphenyl-1-picrylhydrazyl (DPPH) radical scavenging activity assay according to modified method presented in [19] with ascorbic acid as a standard. DPPH-scavenging activity of 25 µL of methanolic extracts was measured by incubation with 200 µL of 0.2 mM DPPH radical for 40 minutes and the absorbance [A] was measured at 515 nm. The percentage of radical scavenging [%Quenching] was calculated using the following formula: Q[%]=[Ablank-Asample]/Ablank×100.

2.6. LC-MS analysis

Methanolic extracts for LC-MS analysis were prepared according to [20]. LC-MS system consisted of UPLC with a photodiode-array detector PDAeλ (Acquity System; Waters) hyphenated to a high-resolution Q-Exactive hybrid MS/MS quadrupole Orbitrap mass spectrometer (Thermo Scientific, http://www.thermofisher.com/). Chromatographic profiles of metabolites and the quantitative measurements were obtained using water acidified with 0.1% formic acid (solvent A) and acetonitrile (solvent B) with a mobile phase flow of 0.35 ml/min on a ACQUITY UPLC HSS T3 C18 column (2.1 × 50 mm, 1.8 µm particle size; Waters) at 22°C. The injection volume was 5 µl.

Q-Exactive MS operated in Xcalibur version 3.0.63 with the following settings: heated electrospray ionization ion source voltage −3 kV or 3 kV; sheath gas flow 30 L/min; auxiliary gas flow 13 L/min; ion source capillary temperature 250°C; auxiliary gas heater temperature 380°C. MS/MS mode (data-dependent acquisition) was recorded in negative and positive ionization, at resolution 70000 and AGC (ion population) target 3e6, scan range 80 to 1000 *m/z*.

Obtained LC-MS data was processed for peaks detection, deisotoping, alignment and gap filling by MZmine 2.51 [21] separately for positive and negative ionization mode, then

Preprints (www.preprints.org) | NOT PEER-REVIEWED | Posted: 26 July 2022 doi:10.20944/preprints202207.0378.v1

data from both modes was combined. Signals corresponding to mycotoxins identified in LC-MS/MS on the basis of literature data, databases and fragmentation spectra were removed from analysis (Table S1). Prepared data table was post-processed for missing values imputation, log transformation and data filtering for further statistical analysis. Datasets from positive and negative ionization are deposited in a publicly available database Metabolights with accession numbers MTBLS1748 (the URL www.ebi.ac.uk/metabolights/MTBLS1748).

2.7. Statistical analysis

Processed LC-MS data set consists of 5 experimental groups (genotypes) in 2 treatments (control and infection), 2 time points (T1,T2), 4 biological replications and 2 experiments for 16781 signals for negative ionization and 8132 signals for positive ionization. Observations equal to zero (below the detection level) were substituted by half of the minimum non-zero observation for each signal. Then observations were transformed by logarithmization in order to bring the data distribution close to a normal distribution. Three-way analysis of variance (ANOVA) was done with experiment as a block (random effects) and treatment, genotype, time point as 3 fixed factors. Statistical analysis was performed together for positive and negative ionization. The resulting p-values were corrected for multiple testing by calculating q-value (the false discovery rate, FDR). Significant changes in accumulation of metabolites were indicated for the effect of treatment, for the effect of genotype, for the effect of time points and all its possible interactions with q-value < 0.05 (Table. 1).

Deferentially accumulated metabolites (DAMs) between inoculated and control plants for each species in each time point, were selected with the following conditions: if any effect containing treatment was significant (treatment or interaction treatment x species or interaction treatment x time point or interaction treatment x species x time point) with q-value < 0.05 and $|\log2FC|>0.58$, where FC is the the fold change equal to treatment/control for each species in each time point. The tables containing results of ANOVA and DAMs selection are available at Table S2.

ANOVA was done in Genstat 21. The false discovery rate was calculated in R 4.0.4. Visualizations including PCA, heatmaps, Venn diagrams, dendrograms and barplots were created in R 4.0.4. PCA was done for each time point on the data after logarithmic transformation and the fold change calculation (log2FC) only for DAMs, Venn diagram for different time points were done on DAMs for each genotype. Dendrograms were done on means in 4 variants, for control at T1, for control at T2, for infection at T1 and for infection at T2. Barplots were done on the number of DAMs for each genotypes and time point. Heatmaps showing differences between treatment and control for each time point and for each genotypes were done on log2FC values for 35 significant DAMs selected from whose with any effect containing treatment significant with q-value<0.01 and with 5 greatest values of $|\log2FC|$ for each species in each time point, not taking account repeated metabolites among genotypes. Observe, that

$\log_2\langle\langle FC=\rangle\rangle \log_2\langle\langle treatment/control\rangle\rangle=\log_2\langle\langle treatment-\log_2 control\rangle\rangle$,

which means that heatmaps were done on differences between preprocessed treatment and control. Moreover, some interesting DAMs from biological point of view were also presented. Heatmaps showing differences between treatment and control for each time point for DAMs share between resistant as well as susceptible genotypes were done on log2FC values for significant DAMs selected from whose with any effect containing treatment significant with q-value<0.01 were common for Tr and Hr and was not DAMs in other genotypes, and consequently common for Ts and Hs but not DAMs in other genotypes.

Four correlation networks: separately for each time point in control and treatment were constructed by WGCNA package in R [22] and visualized by Cytoscape [23]. First Pearson correlation matrix was transformed into an adjacency matrix using a power

 doi:10.20944/preprints202207.0378.v1

function 6 in all cases according to the scale-free topology criterion [22]. Modules were detected by clustering using the dynamic tree cut algorithm on the topological overlap matrix, which was visualized via Cytoscape. For all networks, hubs, defined as highly connected metabolites were selected as nodes with the highest number of connections.

2.8. Functional analysis and metabolites characterization

Signals selected as DAMs were combined from positive and negative ionization and were imported to Functional Analysis module in MetaboAnalyst 5.0 [24] as a peak list profile. Annotation was done with 5 ppm mass tolerance and Mummichog algorithm with 0.05 p-value cutoff on the basis of *Oryza sativa japonica* (Japanese rice) reference metabolome in KEGG: Kyoto Encyclopedia of Genes and Genomes [25] The annotated compounds were subsequently subjected to Pathway Analysis and Enrichment Analysis modules in MetaboAnalyst 5.0 for pathway enrichment and structural enrichment, respectively. Metabolites over-represented on pathway level was ranked on the basis of hypergeometric test followed by Benjamini-Hochberg false discovery rate (FDR) correction. The relative importance of individual nodes to the overall pathway network (pathway topology) was scored on the basis of Relative-betweenness Centrality. Significantly enriched metabolic pathways upon differentiating factors were selected if FDR < 0.03 consistently across multiple comparisons and presented in table 2. The entire result tables containing scoring of pathway mapping for functional annotation and enrichment impact are available in Table S3 for each analysis with two sheets. The sheet entitled "pathway enrichment" contains scoring of entire pathway enrichment for all experimental groups. The sheet entitled: "annotation" contains information about annotated metabolites with databases KEGG [25], HMDB [26], PubChem [27]. Metabolites over-represented by structural classification were ranked on the basis of metabolite set enrichment analysis (MSEA) grouping with FDR < 0.01. The significant enrichment by structural classification results were also presented in table 2 and entire result table containing scoring of structural mapping is available in Table S4.

Individual DAMs annotation from enrichment analysis was complemented by tentative DAMs identification on the basis of *m/z* value, fragmentation in MS/MS spectra and confirmed via comparison of the exact molecular masses with Δ less than 5 ppm, retention times and mass spectra to those of standard compounds or spectra in available databases (PubChem, ChEBI, Metlin, Reaxys and KNApSAck, ReSpect) [28]; [29]; [30]; [27] [31] and literature data. The confirmation of aglycone type of flavonoid isomers (e.g. kaempferol and luteolin differentiation) was based on standard compounds comparison and method described previously [32].

3. Results

3.1. FHB disease severity was diversified among genotypes

Genotypes of barley and wheat characterized as susceptible to FHB had the higher level of fungal biomass than resistant ones. It should be noted that in Ts biomass of *F. culmorum* was much more expanded than in Hs (Figure 1 A). Fungal biomass in Bd was at similar level as for Hs and more expanded than in resistant genotypes. Differences in biomass production between both wheat cultivars were prominent with statistical significance $p < 0.05$ hereas both barley genotypes manifested moderate differences.

3.2. Antioxidant capacity was triggered in susceptible but not in resistant genotypes

The total antioxidative activity was evaluated on in vitro methanolic extracts of studied plants. In resistant genotypes the antioxidant capacity was similar in control and infected plants (Figure 1 B). In Hs the antioxidant capacity decreased slightly while in Ts and Bd the decreasing was significant. Interestingly in control plants Tr antioxidant capacity was constitutively lower than in other studied grasses.

3.3. Resistant genotypes impaired mycotoxin production by F. culmorum

 doi:10.20944/preprints202207.0378.v1

Genetic characterization of *F. culmorum* strain revealed expression of genes related to production od mycotoxins from trichotecene and estrogen classes (Table S5). In vitro assay shown relatively higher level of genes expressions for estrogenic zearalenone (ZEA synthase -ZEA2) than trichotecenes (Zinc finger transcription factor -*TRI6*, Trichodiene synthase – *TRI5*). Global LC-MS analysis enabled to detect five mycotoxins: zearalenone (ZEN), nivalenol (NIV), deoxynivalenol (DON), diacetoxyscirpenol (DAS) and T2 toxin on the basis of *m*/*z* value and fragmentation spectra according to [33]. Type A-trichothecenes including DAS and T2 toxin were detected with positive ionization mode as ammonium adduct $[DAS+NH_4]^+$, $[T\text{-}2+NH_4]^+$ ions at *m*/*z* =384.2022 Da and 484.2546 Da, respectively,(Figure S1 and Table S1). For type B-trichothecenes NIV and DON the respective precursor $[NIV+CH_3COO]^-$ and $[DON+CH_3COO]^-$ ion represented adducts with formic acid at m/= 371.1342 Da and *m*/*z*=355.1392, respectively. Estrogenic zearalenone detection was on the basis of [M-H]- ion at *m*/*z*= 317.1472624 Da. These signals were removed from data table serves for statistics for visualization of plant immunity response (described in 3.4.). Processed and normalized data enable for comparison of accumulation of detected mycotoxins. Diacetoxyscirpenol significantly accumulated in both barley genotypes, while nivalenol was more pervasive in wheat genotypes (Figure 1 C-G). T2 toxin was close to detection limit in resistant genotypes Tr and Hr. Susceptible genotypes Ts and Hs had high level of T2 toxin accumulation and the highest level was shown for Bd21. Interestingly, trend of accumulation for other detected mycotoxins in Bd21 was similar to susceptible genotypes except for zearalenone which trend of accumulation was close to resistant genotypes. Time point of mycotoxins measurement had weak effect on mycotoxins accumulation and the level was stable from T1 to T2.

Processed LC-MS data cannot give quantitative results, therefore, the most accumulated mycotoxin of *F. culmorum* strain used in our experiments zearalenone was quantitatively measured in spikes on the basis of UV calibration curve. Quantitative measurement of ZEA shown the same kinetic of accumulation as detected by LC-MS. Resistant variants of barley and wheat were characterized by significantly lower level of zearalenone, (less than 10 ng/g of dry weight) in comparison to susceptible plants (Figure 1 H). Results obtained for Bd, (14 ng/g of dry weight), were close to the results for resistant variants. Large discrepancies in the results for susceptible genotypes were observed. The highest level of zearalenone was detected in Ts (about 150 ng/g of dry weight) and it was almost 10 time prevalent level than in Tr. It is worth to mention that UE norm for zearalenone accumulation in spikes is 100 ng/g (100 ppb).

Preprints (www.preprints.org) | NOT PEER-REVIEWED | Posted: 26 July 2022 doi:10.20944/preprints202207.0378.v1

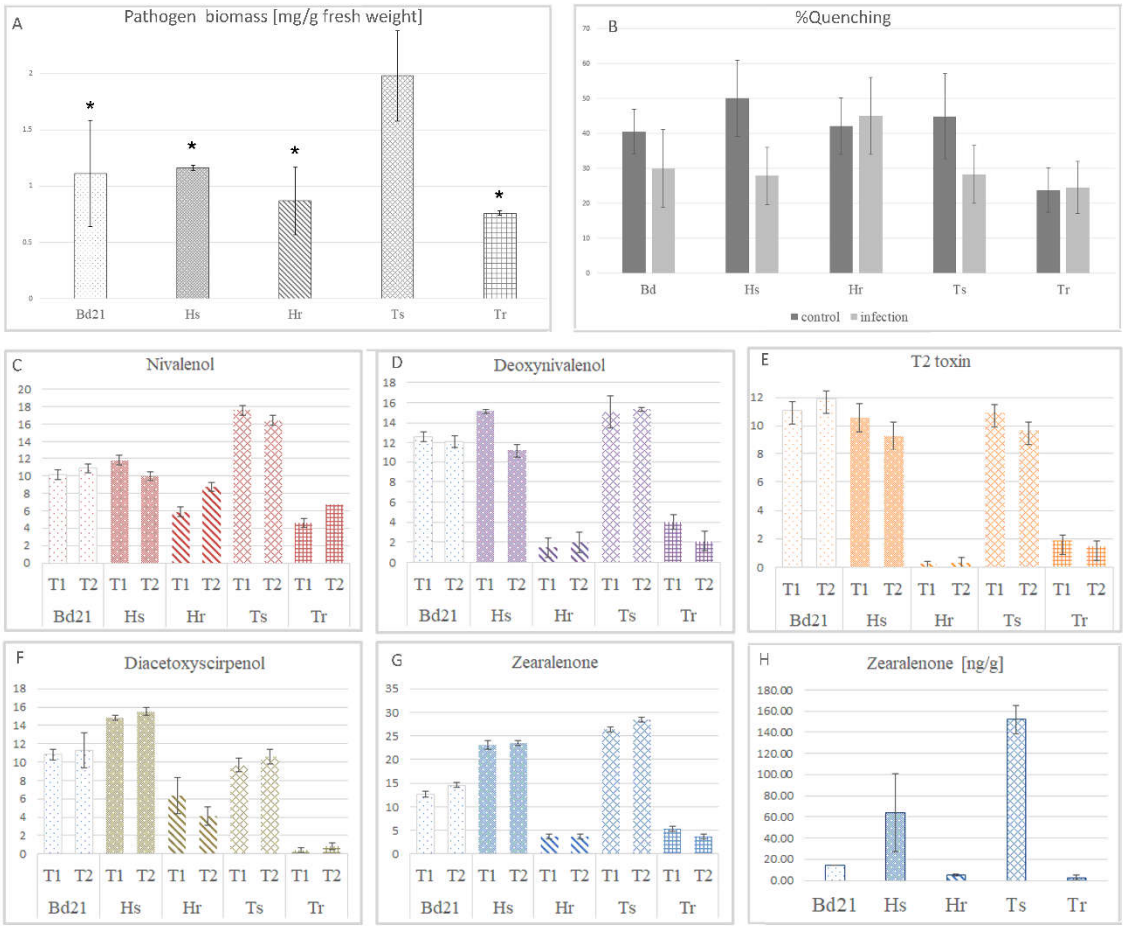

Figure 1. Progress of pathogenesis in different genotypes of Poaceae measured by (A) *Fusarium culmorum* biomass quantified by real-time qPCR assay. Significant differences between susceptible and resistant plants using Student's t-test: * p-value<0.05; (B) DPPH radical scavenging capacities of the methanolic extracts of plants expressed as nM trolox equivalent (TE) per 100 g of extract;(C) LC-MS measurement of nivalenol accumulation at T1 and T2; (D) LC-MS measurement of deoxynivalenol accumulation at T1 and T2; € LC-MS measurement of T2 toxin accumulation at T1 and T2; (F) LC-MS measurement of diacetoxyscirpenol accumulation at T1 and T2; (G) LC-MS measurement of zearalenone accumulation at T1 and T2; (H) Quantitative measurement of zearalenone accumulation [ng/g dry weight] in infected plants at T2; In C-H results for control plants were skipped as the level of mycotoxin was close to or under the detection limit; D. Symbol "Bd" is for *Brachypodium distachyon* Bd21 line, "Hs" is for *Hordeum vulgare* FHB - susceptible genotypes, "Hr" is for *Hordeum vulgare* FHB - resistant genotypes, "Ts" is for *Triticum aestivum* FHB - susceptible cultivar and "Tr" is for *Triticum aestivum* FHB - resistant cultivar.

3.4. Conserved DAMs were highly correlated while genotype-specific DAMs determined variation in resistance to FHB

Our three factorial experimental set up included three factors: genotype, treatment and time point, therefore required sophisticated method of three-way ANOVA for realistic significance of signals for all three factors and their interactions. The highest number of significant signals was for genotype factor - 19596 significant signals among 24913 all signals taken for analysis (Table 1). Interactions between genotype and other factors were numerous, especially interactions between genotype and time points. The effect of interactions between treatment and time points was the lowest. Triple interaction treatment x genotype x time points was also meaningful.

Preprints (www.preprints.org) | NOT PEER-REVIEWED | Posted: 26 July 2022 doi:10.20944/preprints202207.0378.v1

Table 1. Number of statistically significant LC-MS signals as a result of three-way analysis of variance followed by the false discovery rate correction.

Effect	Number of significant metabolites with q-value < 0.05
treatment	3935
genotype	19596
time points	5628
treatment x genotype	5001
treatment x time points	271
time points x genotype	9941
treatment x genotype x time points	1874

The calculation of the fold change between inoculated and control plants complimented by selection of statistically significant signals by ANOVA enabled to select Deferentially Accumulated Metabolites (DAMs) to indicate metabolites common for all genotypes and genotype-specific in immune response of Poaceae plants (Table S2). Strong metabolomic response to *F. culmorum* inoculation was observed in all studied genotypes since thousands of signals had changed accumulation between controls and inoculated groups (Figure 2 A). Even at early infection stage at T1 number of signals with increased or decreased accumulation was more than two thousand for every genotype. At T2 number of DAMs significantly increased for every genotype. Proportionally lesser changes were observed for barley genotypes whereas wheat and Bd had extended number of DAMs with increased and decreased accumulation. In wheat and Bd the differences in DAMs number was more evident, especially for DAMs with decreased accumulation. The lowest number of DAMs with the least variable from T1 to T2 was observed in barley genotypes. Metabolomic profile of Bd21 control plants was close to wheat control plants, especially to resistant Tr, whereas both barley genotypes were distant to each other and the rest studied genotypes (Figure 2 B). The reprogramming due to response to FHB caused approximation of the metabolome profiles between Bd21 and barley genotypes at both time points (Figure 2 C). At T2 the metabolomic profiles of all plant genotypes shifted to higher inter-species distance.

Preprints (www.preprints.org) | NOT PEER-REVIEWED | Posted: 26 July 2022 doi:10.20944/preprints202207.0378.v1

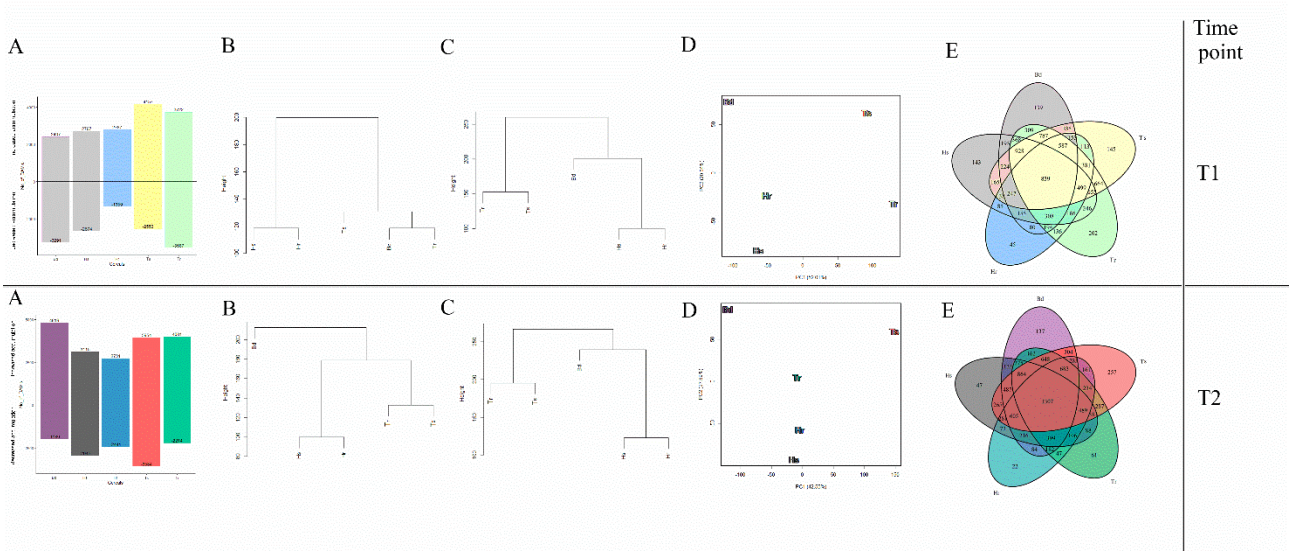

Figure 2. Characterization of global metabolomic changes in studied genotypes in response to *F. culmorum.* Upper panel representing results for time point T1 and bottom panel representing results for time point T2 (A) Bar charts presenting number of DAMs selected after ANOVA with q-value < 0.05 and fold change (FC) between inoculated and control group |log2FC|>0.58 with increased or decreased accumulation after *F. culmorum* inoculation in each genotype, (B) hierarchical clustering of metabolomic profile for control plants on the basis of Euclidean distance and complete link grouping algorithm, (C) hierarchical clustering of metabolomic profile for group of plants infected with *F. culmorum*, (D) PCAs of DAMs for studied genotypes, (E) Venn diagrams presenting number of shared and unique DAMs for studied genotypes. Symbol "Bd" is for *Brachypodium distachyon* Bd21 line, "Hs" is for *Hordeum vulgare* FHB - susceptible genotypes, "Hr" is for *Hordeum vulgare* FHB - resistant genotypes, "Ts" is for *Triticum aestivum* FHB - susceptible cultivar and "Tr" is for *Triticum aestivum* FHB - resistant cultivar.

Overall, metabolomic immune response to FHB was diversified among all tested genotypes (Figure 2 D). DAMs of Bd21 had the highest distance to other groups at both time points. DAMs of barley and wheat showed more intra-species similarities from T1 to T2. In spite of differences in metabolomic profile, the conservatism of the responses among all tested genotypes was significant. Common DAMs observed at later stage of infection at T2 (1307 common signals) was greater than at T1 (839 common signals) (Figure 2 E). Elements specific only for susceptible or resistant genotypes can be also observed. Tr and Hr had 136 shared DAMs at T1. The number decreased to 47 at T2. On the other hand, Ts and Hs had 165 shared Dams at T1 and the number increased at T2 to 265. Bd21 has the higher number of shared DAMs with wheat genotypes. At T1 there were 309 shared DAMs between Bd21 and Tr, whereas at T2 higher commonality showed with Ts (304). Both barley genotypes shared significantly less number of DAMs than wheat genotypes. There was 85 and 73 DAMs shared for barley genotypes at T1 and T2, respectively, in comparison to 664 and 287 DAMs at T1 and T2, respectively shared for both wheat genotypes.

Due to large number of common DAMs we checked the correlation networks among them in control and after FHB progress. Those signals had low level of connectivity at both time points for control conditions while biotic stress caused increasing of correlation between particular DAMs (Figure 3 for T2 and Figure S2 for T1). Upon infection correlation became more intricate and extending beyond modules. The most numerous turquoise module at control conditions divided into two modules turquoise and lightcyan after *F. culmorum* inoculation due to enhancement of correlations among particular DAMs. The inter-modular connectivity became noticeable especially for unsaturated fatty acids and phenylpropanoids. DAMs with the highest number of connection assigning as hubs was predominantly hydroxycinnamic acids incorporated to the biggest turquoise module. Ferulic acid and two isomers of *p*-coumaric acid glucoside had 135, the highest number of

 doi:10.20944/preprints202207.0378.v1

connection to other DAMs. Derivatives of sinapic and ferulic acid also belonged to strongly correlated DAMs. (Epi)catechin isomers and naringenin from flavonoids structure were also highly connected metabolites in this module. Other flavonoid, dihydromorin was the only one hub of cyan module with mainly positive correlation to other DAMs. The highest number of hubs belonged to purple module in which flavonols, apigenin and tricin, ferulic acid derivative and phosphorylated thymidine were correlated between each other. Jasmonic acid shown strong intra-modular negative correlation. However, its derivative MeJa had strong positive correlation within the cyan module. Lightgreen module enriched relatively high number of positively correlated hubs with mainly annotation to sphingosine and unsaturated fatty acids.

Preprints (www.preprints.org) | NOT PEER-REVIEWED | Posted: 26 July 2022 doi:10.20944/preprints202207.0378.v1

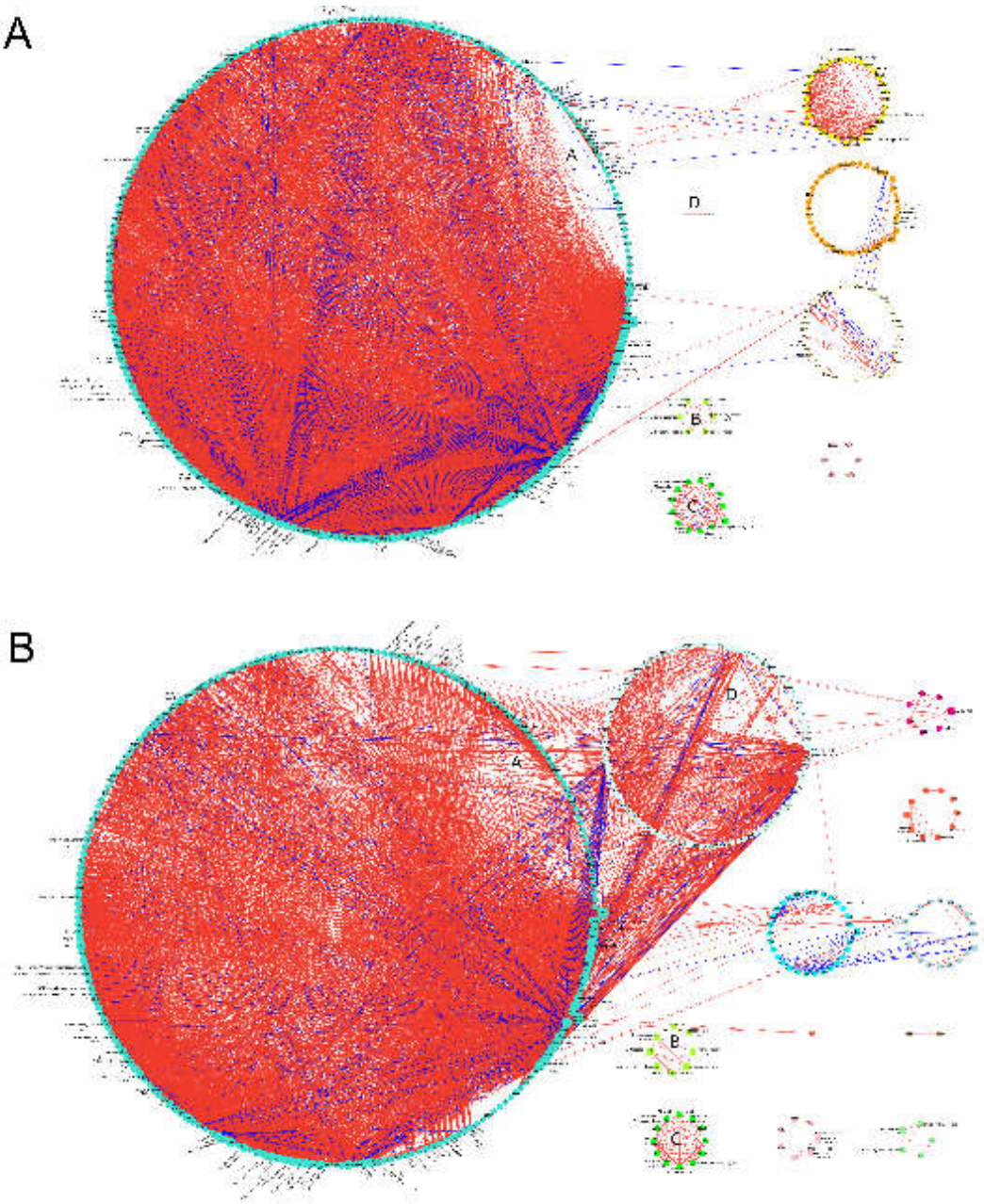

Figure 3. The correlation network of metabolites observed (A) at T2 in control conditions, (B) at T2 after *F. culmorum* inoculation. Metabolites are represented by circles with numbers. The size of the circle is proportional to the number of edges/connections created by this compound. Squares denote hubs, i.e., compounds with the highest number of connections. Edges link highly correlated metabolites. Modules of metabolites are visualized by different colors. Only edges corresponding to elements of the topological overlap matrix greater than 0.25 are shown, both within and between modules, red edges—positive correlations, blue edges—negative correlations. The modules with a large number of metabolites (>60%) occurring in both control and treatment are marked with letters (A)–(D).

3.5. Evolutionary conserved metabolic pathways enriched common DAMs

Firstly, all common DAMs presented at Venn Diagram (Figure 2 E, 839 at T1 and 1307 at T2) were subjected to enrichment analysis by annotation to KEGG pathway database (https://www.genome.jp/kegg/pathway.html). The metabolic pathways with the highest score of enrichment were selected for functional analysis (Table 2 and Tables S3). For confirmation and extension of results from enrichment analysis, the same sets of signals were subjected to metabolomic data bases search followed by MS/MS spectra inspection prior

 doi:10.20944/preprints202207.0378.v1

to confirmation of proper annotation. Additionally, the annotated metabolites were grouped according to structural classes.

"Galactose metabolism" had the highest score of enrichment at T1 and T2 (Table 2) among common DAMs on the basis of FDR significance and pathway impact. Most of the annotated compounds belonged to module of "Raffinose family oligosaccharides". Also photosynthesis-related "Porphyrin and chlorophyll metabolism" was enriched at both time points and incorporated metabolites from "Heme biosynthesis" module. Phenylpropanoids were the most numerous annotated group of metabolites at both time points. Functional annotation on the basis of KEGG shown "Phenylpropanoid biosynthesis" pathway at T1 incorporating *p*-coumaric, caffeic, ferulic and sinapic acids and their aldehyde derivatives. At T2 spermidines conjugated with hydoxycinnamic acids and monolignols (annotated as syringin and coniferin and derivatives) were additionally matched. Dominant DAMs at T1 characterized by additional databases searching were derivatives of apigenin, kaempferol, quercetin and chalcones from "Flavonoids biosynthesis". Differently, at T2 only one flavonoid, pentahydroxyflavanone was determined. Pathways related to aromatic amino acids from "Tyrosine metabolism" at T1 and "Tryptophan metabolism" at T2 were also commonly changed in grasses. Highlighting tryptophan-derived metabolites at T2 was complimented by databases annotation of indoleacetic acid and its 5-hydroxylated form as well as tryptamine and *N*-salicyloyltryptamine. Ascorbic acid was matched as central metabolite from "Ascorbate and aldarate metabolism". Unsaturated fatty acids from "Arachidonic acid metabolism", but not arachidonic acid themselves and central regulatory "2-Oxocarboxylic acids" were triggered at T2. Diversification of chemical structures of DAMs through infection progress from T1 to T2 reflects structural classification. At T1 enrichment with FDR <0.01 was for 16 metabolite classes while at T2 the number was increased to 20 classes (Table 1 and Table S4). Grouping annotated signal on the basis of structural classes by MSEA enrichment confirms the strong changes among benzamides, monosaccharides, isoprenoids, purines and pirimidines, TCA acids, amino acids and peptides and porphyrins at both time points.

Preprints (www.preprints.org) | NOT PEER-REVIEWED | Posted: 26 July 2022 doi:10.20944/preprints202207.0378.v1

Table 2. Enrichment analysis of LC-MS signals annotated to KEGG Metabolic pathways and structural groups selected as the most enriched for DAMs visualized in Venn Diagram in Figure 2E. Only pathways with FDR of matching<0.3 and pathway impact I>0.5 were presented in table as statistically significant. Entire functional enrichment results and compounds annotation can be found at Table S3. Only structural classes enriched with FDR of matching< 0.01 were presented in table as statistically significant. Entire structural enrichment results can be found at Table S4.

genotype	Time point T1		Time point T2	
enrichment	functional	structural	functional	structural
common	Galactose metabolism	Benzamides	Galactose metabolism	Benzamides
	Porphyrin and chlorophyll metabolism	Monosaccharides	Ascorbate and aldarate metabolism	Purines
	Flavonoid biosynthesis	Amino acids and peptides	Porphyrin and chlorophyll metabolism	Amino acids and peptides
	Phenylpropanoid biosynthesis	Purines	Arachidonic acid metabolism	Monosaccharides
	Tyrosine metabolism	Porphyrins	2-Oxocarboxylic acid metabolism	Isoprenoids
	Isoquinoline alkaloid biosynthesis	TCA acids	Tryptophan metabolism	Indoles
		Pyrimidines	Phenylpropanoid biosynthesis	Porphyrins
		Cinnamic acids		Pyrimidines
		Sphingoid bases		Glycosyl compounds
		Pyridoxamines		Cinnamic acids
		Benzenes		TCA acids
		Fatty Acids and Conjugates		Sphingoid bases
		Short-chain acids and derivatives		Benzenediols
		Isoprenoids		Tryptamines
		Disaccharides		Disaccharides
				Eicosanoids
		Benzenediols		Imidazoles
				Phenols
				Organooxygen compounds
				Aldehydes
Hs	Biosynthesis of secondary metabolites - other antibiotics	Benzamides	Biosynthesis of secondary metabolites - other antibiotics	Monosaccharides
	Galactose metabolism	Amino acids and peptides	Diterpenoid biosynthesis	Disaccharides
	Ascorbate and aldarate metabolism	Porphyrins	alpha-Linolenic acid metabolism	Purines
	alpha-Linolenic acid metabolism	TCA acids	Arachidonic acid metabolism	
	Diterpenoid biosynthesis	Monosaccharides		
		Isoprenoids		
Hr	Arginine and proline metabolism	Amino acids and peptides	Caffeine metabolism	Purines
	2-Oxocarboxylic acid metabolism	Benzamides	2-Oxocarboxylic acid metabolism	
	Phenylpropanoid biosynthesis		Purine metabolism	
Ts	Biosynthesis of secondary metabolites - other antibiotics	Purines	Arachidonic acid metabolism	Benzamides

Preprints (www.preprints.org) | NOT PEER-REVIEWED | Posted: 26 July 2022 doi:10.20944/preprints202207.0378.v1

	Arachidonic acid metabolism	Benzamides	Diterpenoid biosynthesis	Amino acids and peptides
	Caffeine metabolism	Monosaccharides		Monosaccharides
	Amino sugar and nucleotide sugar metabolism	TCA acids		Quinones and hydroquinones
		Imidazoles		Sterols
		Amino acids and peptides		Cyclic alcohols
		Indoles		Tryptamines
		Eicosanoids		Isoprenoids
				Benzoic acids
				Pyrimidines
				Fatty Acids and Conjugates
				Purines
				Cinnamic acids
				Eicosanoids
Tr	Flavonoid biosynthesis	Benzamides	Biosynthesis of secondary metabolites - other antibiotics	Benzamides
	Flavone and flavonol biosynthesis	Purines	Cutin, suberine and wax biosynthesis	
	Arachidonic acid metabolism	Monosaccharides	Linoleic acid metabolism	
	Phenylpropanoid biosynthesis	Imidazoles	Biosynthesis of unsaturated fatty acids	
		Cinnamic acids	Arachidonic acid metabolism	
		Isoprenoids	Galactose metabolism	
		Eicosanoids	alpha-Linolenic acid metabolism	
		Flavonoids		
Bd21	Amino sugar and nucleotide sugar metabolism	Monosaccharides	Phenylpropanoid biosynthesis	Purines
	Glycolysis / Gluconeogenesis	Benzamides	Purine metabolism	Pyrimidines
	alpha-Linolenic acid metabolism	TCA acids	Linoleic acid metabolism	Phenylpropanoids
	Pentose phosphate pathway	Purines	Flavone and flavonol biosynthesis	
	Fructose and mannose metabolism	Phosphate esters		
	Citrate cycle (TCA cycle)			
	Galactose metabolism			
	Inositol phosphate metabolism			
	Glyoxylate and dicarboxylate metabolism			
	Carbon fixation in photosynthetic organisms			

3.6. Pathways used four-nitrogen containing metabolites and amino acids can accelerate resistance of barley genotype

Similar FHB-related pathways were triggered at both time points in Hs genotype. The enrichment concerned lignan biosynthesis of matairesinol and secoisolariciresinol (in KEGG incorporated to "Biosynthesis of secondary metabolites - other antibiotics") as well as "α-Linolenic acid metabolism", and gibberellin biosynthesis pathway from "Diterpenoids metabolism". Specifically at T2 DAMs from "Arachidonic acid metabolism" were matched while at T1 "Ascorbate and aldarate metabolism" was triggered.

The best score for Hr at T1 was for metabolism of amino acids and derivatives from "Arginine and proline metabolism" and phenolics from "Phenylpropanoid biosynthesis".

Preprints (www.preprints.org) | NOT PEER-REVIEWED | Posted: 26 July 2022 doi:10.20944/preprints202207.0378.v1

"2-Oxocarboxylic acid chain extension" pathway was represented at both time points by sulphur-containing dicarboxylic acids methylthiopentylmalic acid isomers at T1 and methylthiobutylmalic acid isomer at T2. Other matched metabolites belonged to flavonoids, mainly glycosidic forms of flavonols. In further stadium of infection at T2 four-nitrogen containing metabolites were annotated as can be suggested from "Caffeine metabolism" and "Purine metabolism" enrichment. In "Caffeine metabolism" annotation of paraxanthine and theobromine which are transformed to 1,7-dimethyluric acid and 3,7-dimethyluric acid, respectively was shown. In second mentioned "Purine metabolism" pathway adenosine, deoxyguanosine and allantoic acid were annotated. Interestingly, cAMP and GMP were matched at T1 and T2, respectively.

Structural over-representation of DAMs for Hs indicated on 6 metabolite classes at T1 with reduction of the number to 3 of number at T2 representing predominantly saccharides and purines. Amino acids and peptides together with benzamides were selected at T1 while only purines a were selected at T2 for Hr.

3.7. Pathways related to unsaturated fatty acids and cell wall biopolimers were enriched in resistant wheat

Ts similarly to Tr significantly changed "Arachidonic acid metabolism" during FHB. However, the arachidonic acid themselves were not annotated as DAMs. Lignan pinoresinol and their derivatives detected at T1 were matched to "Biosynthesis of secondary metabolites - other antibiotics". Enriched "Caffeine metabolism" is related to metabolites with purine ring. Mono- and di-terpenes skeleton was mainly related to "Gibberellin A12 biosynthesis" module. Moreover, sesquiterpene derivatives of abscisic acid as well as dicarboxylic acids, thiamine monophosphate (vitamin B1) and porphobilinogen were also matched at T2 thanks to additional databases searching.

In Tr at T1 phenolics-related pathways were mainly enriched. Additional databases searching revealed prevalence of different hydroxycinnamic acids. Complex isomeric structures as dicaffeoylquinic acids at T1 and conjugates with polyamines as coumaroylagmatine and caffeoyl-putrescin at T2 were observed. An equally large class constituted flavonoids represented by chalcones, flavones, flavanones and flavanols. Interestingly, matched compounds from this structural class contained numerous methylations and prenylation in their core aglycon. Pathways predominant in Tr at T2 incorporating unsaturated fatty acids and phospholipids. Steroidal structure of cholic acid and their conjugates were also characteristic DAMs for wheat. Those molecules in cooperation with glycerols and phenolics serve as precursor for "Cutin, suberine and wax biosynthesis" which changes was also FHB-related in Tr.

3.8. Bd 21 induced pathway of bioenergetics governing in response to F. culmorum

DAMs enriched for Bd21 differed significantly between both time points. At T1 annotated metabolites belonged predominantly to pathways responsible for bioenergetic supply "Citrate cycle (TCA cycle)" and "Glycolysis/Gluconeogenesis". Sugar metabolism linked to "Amino sugar and nucleotide sugar metabolism", "Pentose phosphate pathway" and "Fructose and mannose metabolism" were also FHB-responsive. In addition, to "α -Linolenic acid metabolism" which was enriched at T1, "Linoleic acid metabolism" were matched at T2. Enrichment of DAMs at T2 focused around chlorogenic acid from "Phenylpropanoids biosynthesis", quercetin and kaempferol, flavonols from "Flavone and flavonol biosynthesis" as well as uric acid derivatives from "Purine metabolism" which was strengthened mainly from inosine- and adenine- related compounds. Structural over-representation indicated at T1 on compounds considered as primary metabolites: monosaccharides, TCA acids, purines, phosphate esters, amino acids and peptides as well as amines. In later stage of infection DAMs were classified as benzamides, purines, pyrimidines and phenylpropanoids.

Preprints (www.preprints.org) | NOT PEER-REVIEWED | Posted: 26 July 2022 doi:10.20944/preprints202207.0378.v1

3.9. Predominant DAMs were structurally diversified and exhibited a different, genotype-specific profile of accumulation

In order to find the most differentiated metabolites in studies genotypes we compiled the selected DAMs with the highest changes between control and inoculated plants from particular genotypes separately for T1 and T2 (Figure 4 A, B). There was high diversification in kinetic of particular selected signals at both time points. At T1 flavonoids, purines, pirimidines, amino acids and peptides derivatives were dominated. Flavonoids were DAMs with mainly increased accumulation upon FHB in all genotypes. Catechin isomers had significant increased accumulation with the strongest fold change for Tr. Only B21 at T2 shown decreased accumulation of both catechin isomers. Flavones apigenin and chrysoeriol in addition to methoxyflavone were significant DAMs at T1 while derivatives of other flavones luteolin, acacetin and diosmetin as well as flavonols quercetin and kaempferol were shown as DAMs at T2. Phenylpropanoids appeared among the most differentiating DAMs mainly as hydroxycinnamic acid and their derivatives. *P*-coumaric acid and its conjugates with hydroxyagmatine and galactaric acid had highly diversified accumulation among genotypes and time points. Databases searching revealed hordatines glucosides as DAMs characteristic for barley. Interestingly, signals matched to glucosides of hordatines A, B and C were selected as DAMs instead of hordatines alone.

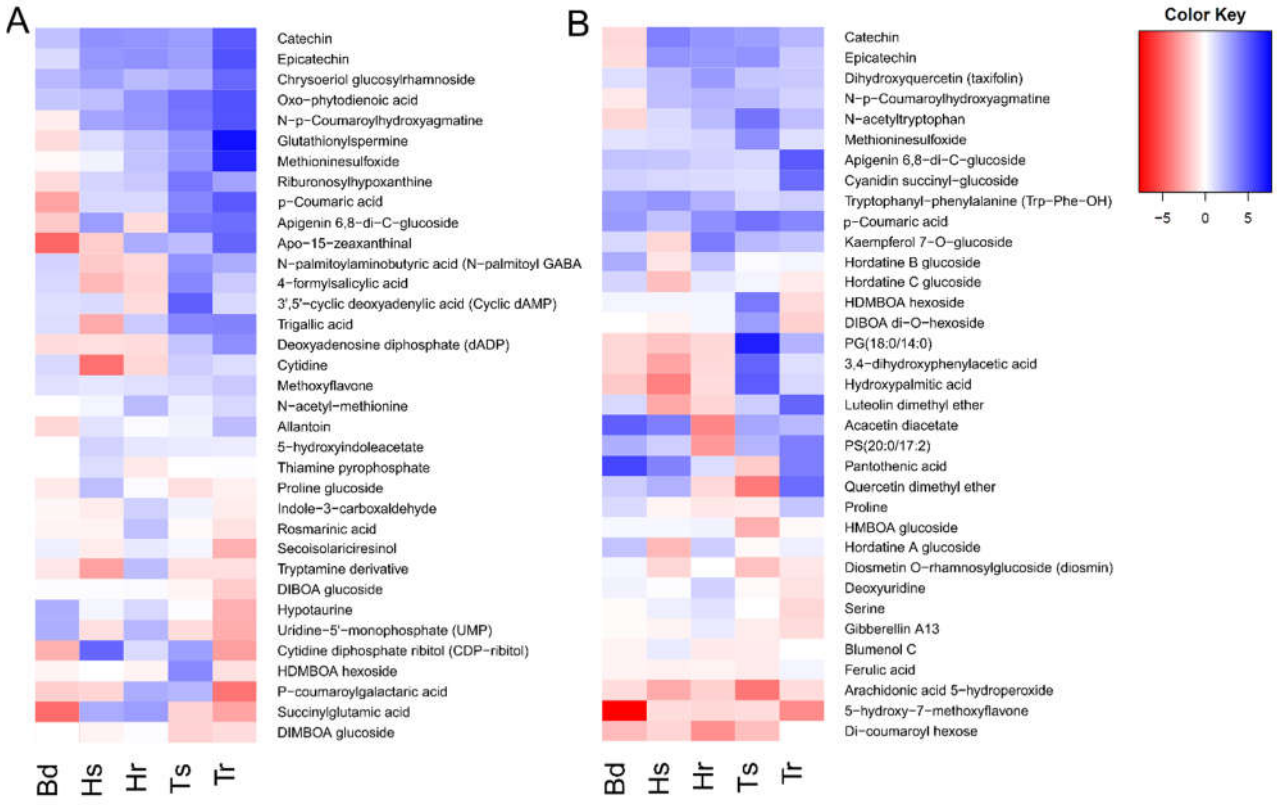

Figure 4. Heatmaps for chosen 35 DAMs highly differentiated among genotypes with tentative annotation on the basis of databases searching for A. T1 time point; B. T2 time point. Symbol "Bd" is for *Brachypodium distachyon* Bd21 line, "Hs" is for *Hordeum vulgare* FHB- susceptible genotypes, "Hr" is for *Hordeum vulgare* FHB- resistant genotypes, "Ts" is for *Triticum aestivum* FHB- susceptible genotype and "Tr" is for *Triticum aestivum* FHB- resistant genotype.

Apart from flavonoids and phenylpropanoids also pirimidines and purines derivatives constituted a numerous group of selected DAMs. 2'-Deoxyadenosine-5'-diphosphate (dADP) has decreased accumulation in Bd21 and barley genotypes whereas increased accumulation in both wheat cultivars. On the other hand cyclic dAMP (2'-Deoxyadenosine cyclic 3',5'- phosphate) decreased only in Hr but opposite changes was observed for other

 doi:10.20944/preprints202207.0378.v1

genotypes. Cytidine diphosphate ribitol (CDP-ribitol) distinguished by high increasing in Hs in comparison to other genotypes.

Unsaturated acids and phospholipids were also selected as DAMs highly responsive to FHB. Arachidonic acid 5-hydroperoxide had decreased while precursor of JA, oxo-phytodienoic acid increased accumulation in all genotypes. The highest increased accumulation of Bd21 was noted for succinylglutamic acid from "Arginine and proline metabolism and apo−15−zeaxanthinal from "Carotenoid biosynthesis".

The principal phytoalexins in wheat as well as rye or maize are specialized metabolites belonged to hydroxamic acids (benzoxazinoids) [4]. Interestingly, only DIBOA glucoside and di-hexoside, DIMBOA glucoside, HMBOA glucoside and HDMBOA hexoside were identified as FHB-related phytoalexins of wheat among benzoxazinoids (Figure 4). However, trend of accumulation was different for all mentioned metabolites. Glucosides of DIBOA and its methylated counterpart DIMBOA shown decreased accumulation in both wheat genotypes. DIBOA di-hexoside shown great increase for Ts while for Tr the accumulation decreased. Similar trend was observed for HDMBOA hexoside. HMBOA glucoside decreased accumulation in both genotypes.

3.9.1. Resistant and susceptible genotypes differed with profile of accumulation of amino acids, pyrimidines, phenolics and JA

In order to check if any metabolite can be related to enhancing FHB-resistance we selected DAMs shared for both Tr and Hr resistant genotypes (Figure 5, Table S6). Relatively high number of DAMs shared for Tr and Hs at the beginning of infection (at T1 was 136 shared DAMs) turned into species-specific metabolic response since only 47 DAMs were selected at T2. Pathway enrichment based on these signals indicated on "Flavonoids biosynthesis", "Arachidonic acid biosynthesis" and "Typtophan metabolism" at T1, while at T2 any significant enrichment cannot be observed. Consequently, we annotated also DAMs common for susceptible genotypes. For T1 and T2, 165 and 265, respectively signals common for Ts and Hs were taken for functional analysis. Any metabolic pathway from KEGG database was significantly enriched at T1 and only two at T2: "Flavonoids biosynthesis" and "Arachidonic acid biosynthesis", probably due to low number of signals taken for analysis. Databases annotation revealed large discrepancies between specific DAMs from T1 and T2 since no metabolites recurred between T1 and T2. Interestingly, databases searching deploys *S*-containing metabolites, sulfanilides and methioninesulfoxide as shared DAMs for resistant genotypes. (Figure 5). However, amino acid methionine was detected as DAMs for susceptible genotypes. Amino acids proline and its glucoside as well as serine were also DAMs for resistant genotypes. Methoxylated and hydroxylated forms of indole-3-acetic acid was found at T1 as resistance-related DAMs. Similarly, methoxylated and hydroxylated forms of flavones were matched. Moreover, prenylation and methylation of variety of flavonoid structures were also observed. Hydroxycinnamic acid shared in Tr and Hr were mainly presented as conjugates with phenolic compounds as in example rosmarinic acid, however, with opposite effect of accumulation between barley and wheat. Lignan secoisolariciresinol was matched as DAMs at T1 for resistant genotypes while other lignans lyoniresinol, pinoresinol and matairesinol were DAMs in susceptible genotypes.

Preprints (www.preprints.org) | NOT PEER-REVIEWED | Posted: 26 July 2022 doi:10.20944/preprints202207.0378.v1

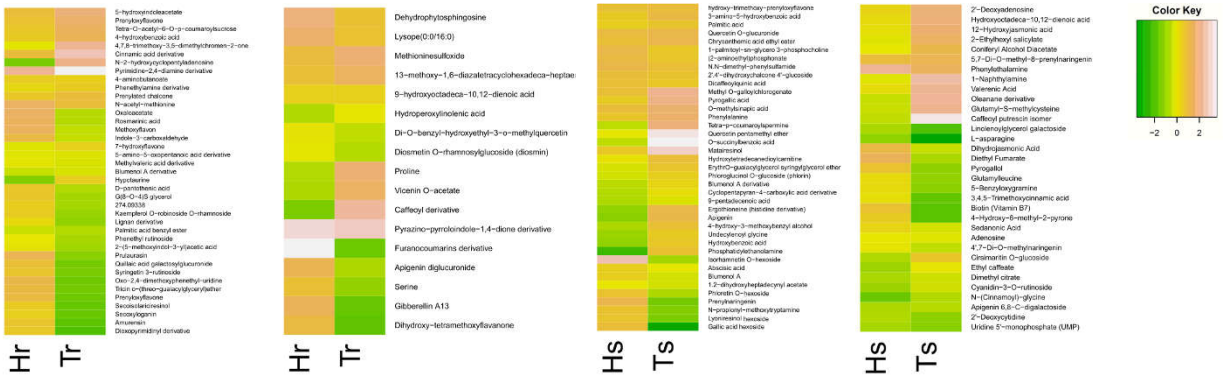

Figure 5. Heatmaps of chosen annotated DAMs shared for FHB-resistant Hr and Tr or FHB-susceptible Hs and Ts genotypes separately for both time points. The details of annotation is available at Table S6. Symbol "Hs" is for *Hordeum vulgare* FHB- susceptible genotypes, "Hr" is for *Hordeum vulgare* FHB- resistant genotypes, "Ts" is for *Triticum aestivum* FHB- susceptible genotype and "Tr" is for *Triticum aestivum* FHB- resistant genotype.

Amino acids phenylanine, histidine but also methionine and asparagine and their derivatives were exclusive DAMs for both susceptible genotypes. There were also indolic methoxytryptamines and gramine derivative in addition to N-acyl amines detected in both time points. Relatively numerous DAMs at T2 belonged to pyrimidines. Among them phosphorylated cytidine, urine and thymidine were matched. In Hs increasing of accumulation was specifically significant for nucleotide derivative cytidine diphosphate ribitol while accumulation of cytidine alone was highly decreased (Figure 4). Prenylated flavonoids, especially chalcones derivatives with two phenyl rings were also observed. Specifically for susceptible plants sesquiterpenoids blumenol A and their derivatives. Derivatives of hydroxycinnamic acids, especially incorporating chlorogenic acid, constitute a numerous group of DAMs shared to susceptible varieties. Interestingly, phytohormones hydroxyjasmonic as well as abscisic acid were also matched among the DAMs common for susceptible genotypes.

4. Discussion

4.1. Infection progress in different genotypes

Fungal growth in Bd21 was at similar level as for Hs, therefore closely resembled of susceptibility to *F. culmorum* between Bd and Hs can be suggested. On the other hand, Bd21 was reported as more resistant to *F. culmorum* then other Bd3-1 ecotype [12]. Taking into account discrepancies in Bd21 reaction to FHB we concluded that this genotype has intermediate resistance to FHB in comparison to selected and well-studied susceptible and resistant genotypes of barley and wheat. Many biological and histopathological studies showed that *F. culmorum*. and *F. graminearum* infect *Brachypodium distachyon* plants in a similar manner as wheat [12]. FHB development and strategy of cells penetration are largely conserved between barley and wheat infection as was observed by [34]. However, wheat cultivars have mostly resistance to the initial penetration (resistant type I) [16], in contrast to barley which has resistance to the pathogen spread within the head (type II) [35]. In addition to comparison between wheat and Bd21 in the response type, similarities in response of barley and Bd were also observed in the signaling pathway for hormones brassinosteroids participating in the F. c. recognition [36].

4.2. Mycotoxins accumulation in spikes

Prior to exclude mycotoxins derived from pathogen from metabolomic studied we compared the *m/z* values and fragmentation spectra based on literature data to signals from our results and removed the corresponding to mycotoxins from statistical analysis.

 doi:10.20944/preprints202207.0378.v1

Without this step signals corresponding to mycotoxins ill be expanded as DAMs from statistical analysis and further influence of functional analysis. In addition to estrogenic zearalenone we detected trichothecene mycotoxins: nivalenol, deoxynivalenol, diacetoxyscirpenol and T2 toxin. Structurally different pathogen-derived metabolites caused slight alterations in transcription patterns in barley and wheat genotypes [37]. Extensive studies on structural dependence of mycotoxins on plant immunity would complete the knowledge of plant-pathogen interaction in FHB.

Bd susceptibilities to *Fusarium* species is DON-dependent [38]. Impact of ZEN on immunity of Bd plant was not clearly described. Moreover, DON contribution in virulence of pathogen was significant in wheat opposite that in barley [39]. Level of accumulation of pathogen-derived metabolites was highly differentiated between resistant and susceptible genotypes and it is positively correlated with pathogen biomass in plants. Similar results was previously described by [40] for wheat and by [41] for barley, where high level of pathogen biomass followed by high level of mycotoxins accumulation. Profile of mycotoxins accumulation in Bd21 was diverse to other species in our experiments. Accumulation of trichotecenes in Bd21 was similar to Ts and Hs whereas estrogenic ZEN accumulation was similar to resistant genotypes. In [38] was noted that the *Fusarium* mycotoxins had the same phenotypic effect in Bd and wheat. *F. culmorum* strain used in our experiments is characterized by low level of DON and high level of ZEN production, therefore the low level of DON can influence on lower level of pathogen biomass accumulation in Bd21. ZEA prevalence can affect the fungal aggressiveness in plant spikes making the description of plant immunity even more challenging.

Apart from comparative LC-MS analyzes of mycotoxins accumulation we measured quantitatively ZEN in order to check if the level of mycotoxins contamination is above adopted safety standards. Moreover, normalization of LC-MS signals caused that it gives only a picture of the kinetics and the trend of mycotoxins accumulation not reflecting the real quantitative results. T1 was established at 4 day and T2 at 8 day after inoculation, respectively. ZEN level exceeded the UE norm only in Ts at T2 but cumulative effect of contamination can be changed over a longer period of research. Nevertheless, the level of mycotoxins accumulation was significant in all genotypes which consistently impact on the physiological and molecular changes in plant after *F. culmorum* inoculation.

4.3. Antioxidant capacity

Secondary metabolism is closely related to plant antioxidative system. Antioxidant capacity and non-enzymatic antioxidants, play a vital role in the detoxification of ROS and photosynthetic balance [42] but also in inhibition of mycotoxin production [43]. We observed that in resistant genotypes of barley and wheat the antioxidant capacity is kept constant even in the advanced stage of *F. culmorum* infection while at the same time increasing the accumulation of secondary metabolites. Compensation of anti-oxidative potential to quench various free radicals generated under FHB by increasing low-molecular antioxidant content was previously observed in different Poaceae plants [44], [45].

H_2O_2 as well as other reactive oxygen species (ROS) is early plant defense response. What is more, mycotoxins produced by Fusarium spp. have been shown to induce H_2O_2 accumulation in the host plant [46]. ROS inhibits the growth of biotrophic pathogens, on the other hands it augments infection process caused by necrotrophic pathogens [47]. *F. culmorum.* as hemibiotrophic with a short biotrophic phase also exert nutritional benefits from dead tissues damaged by ROS [48]. Effective and complex antioxidation system prevents oxidative stress upon elevated ROS and therefore increase resistance to pathogen [49]. In our experiments high efficiency of antioxidative systemin Tr and Hr was manifested by stable level of antioxidative capacity. On the other hand, the weakening of antioxidative activity during *F. culmorum* inoculation in susceptible Ts and Hs is accompanied by a significant increase of the *F. culmorum* biomass suggesting general antioxidant activities as major player in *F. culmorum* spreading. However, unexpectedly, the low level of antioxidative capacity for both control and infected plants of Tr suggests a high efficiency

Preprints (www.preprints.org) | NOT PEER-REVIEWED | Posted: 26 July 2022 doi:10.20944/preprints202207.0378.v1

of these system to overall wheat resistance. Our results indicated on significant role of total antioxidative activities but not antioxidant level in spreading of *F. culmorum*. Similar result was observed previously for resistant and susceptible varieties of wheat [45] and barley [50] in pathogen infection.

4.4. Statistical analysis-added value

Most biological studies deal with only one factor, e.g. with treatment and control, which might be analyzed by one-way ANOVA via many dedicated programs. However, in experiments like in our cases, with more than one factor, those programs do not reflect cumulative effect of the factors. Many non-statistical scientists use programs such as MZmine2, MetaboAnalyst or XCMS which are not suitable for 3-factors or multifactorial experiments. Most experiments are analyzed only by one-way ANOVA like treatment-control data not considering interactions. This way of analysis does not show the real situation, where the results are influenced by the interaction of factors and bring the risk of misleading results. Therefore, we used multivariate statistical analysis methods in our own scripts written in Genstat. According to our knowledge there is no other publication with 3-factor ANOVA and the aim of the analysis as detection of Deferentially Accumulated Metabolites (DAMs). So far, we analyzed metabolomic data using 2-factor ANOVA with additional conditions of the fold change for DAMs selection in [51]. Our advance approach enables to track main effect and effects of interactions among three factors: genotype, treatments and time points followed by the fold change for complementary statistical and biological significance. Our results indicated 1874 signals with significant triple treatment x genotype x time points interaction which cannot be possible to distinct by simplifier ANOVA methods.

4.5. Global analysis

Particular signals detected by LC-MS profiles should not be assigned to individual metabolites. Signal redundancy created by multiple adduct or fragment ions for a single metabolite is phenomena observed for every LC-MS/MS analysis. Nevertheless, the redundancy is decreasing during raw data processing by isotopic peaks removal and adduct with formic acid or sodium removal. Moreover, comparison based on statistically and biologically significant DAMs presenting metabolomic response, not simple comparison of metabolic profile separately for control and infection treatment greatly improve the analysis correctness. We decide to introduce the DAMs definition equal to DEGs, Differentially Expressed Genes, in transcriptomic analysis as we previously applied in [51].

Fusarium-triggered immunological responses involve massive transcriptional reprogramming within hormone, primary metabolism, photosynthesis as well as processes that are essential for plant growth and development [52]). Increased correlation among DAMs confirmed also high reprogramming in metabolome during *Fusarium* infection. High number of DAMs common for all studied genotypes confirm high level of conservativeness of metabolomic response to FHB in Poaceae plants with enhance correlation among. Genotype-specific DAMs can serve for emergence of metabolic biomarker of plant resistance to FHB which are desired for plant breeders for facilitating selection of cultivars with the best immunity properties [53], [54]. On the other hand, the conserved DAMs characterization creates an opportunity to learn about basic molecular processes related to plant immunity.

Dominated effect of genotype and its interaction according to ANOVA had indicating on intra-species diversification in immune response. Differences in metabolic profile among wheat and barley cultivars with diversified susceptibilities to *Fusarium* was previously shown [55], [56]. Resistance to FHB is controlled by many plant quantitative trait loci (QTL) and is highly dependent on morphological traits and environmental conditions [57], [58]. Observed similarities of physiological features between Bd21 and susceptible genotypes of barley and wheat is in opposition to metabolic profile comparison. Bd21 shows intermediate metabolomic FHB-related changes between barley and wheat

 doi:10.20944/preprints202207.0378.v1

metabolome with strong diversification of DAMs. The dispersion of phenotypic and metabolomic features resembling barley or wheat requires clarification. A detailed analysis of the Bd metabolome is necessary to understand the specialized FHB-responsive metabolites, perhaps specific only for Bd.

4.6. Functional metabolomics

Annotation of metabolites via different dedicated databases in context of metabolic pathways brings global look at immunity processes in plants. Many metabolites with changed accumulation during FHB were identified or annotated in Poaceae plants previously (for review see [59]. Nevertheless, their correlation and functionality remains largely unknown. What is more, annotation of particular *m/z* values to dedicated data bases is burdened with a large error due to a isomeric structures and a low degree of metabolome description in Poaceae plants. However, assigning the entire group of compounds to particular metabolic pathway has higher probabilities of correctness than annotation of single *m/z* value. It gives opportunity for DAMs localization into global plant reaction to FHB and grouping metabolite classes. The plant metabolome is highly dependent on external and developmental factors, therefore it is difficult to target the critical ones for plant immunity.

4.7. Conservative metabolomic response to FHB among Poaceae plant

We observed robust enrichment of specific metabolic pathways related to central carbon metabolism and evolutionary conserved phenylpropanoids, flavonoids and porphyrins biosynthesis [60]. Carbohydrates from "Raffinose family oligosaccharides" indicating on disturbance of sugar storage in seeds and germination processes [61]. In addition, galactose-derived oligosaccharides were predicted as antioxidants and ABA-related signaling molecules [62]. Moreover, monosaccharides mannose, galactose and myo-inositol were suggested to increased FHB resistance in wheat [63] and maize [64]. Interestingly, plants from Poaceae family have low level of galactose in cell wall polysaccharides structures, however additional role for galactose in stimulation of phloem import was suggested [65]. As sugar management have been shown to modulate expression of defense-related phenylpropanoids [66] we speculate that the enrichment of these pathways is associated with cascade of signaling leading to reprogramming in secondary metabolome. The observation are underlining by Bd defense response in which sugar management seems to be central part as most of BD21-specific enriched pathway revolves around sugar metabolism. Previous studies on Bd seedlings showed sugar metabolism inductions linked to osmolytes overproduction [67]. Our finding suggested notable function for sugar metabolism in biotic stress response in Bd plants.

Matching at T2 metabolites from central regulatory "2-Oxocarboxylic acids" suggesting disturbances in primary metabolism of TCA cycle and glycolysis [68]. High score of "Porphyrin and chlorophyll metabolism" at both time points corresponded to "Heme biosynthesis" module indicating on large photosynthesis disruption during FHB leading to overproduction of ROS [69] as well as decreasing of chlorophyll content resulting in altered efficiency of photosynthesis [70]. Porhiprins related to conserved FHB response provide via tetrapyrroles precursors to photosynthetic cytochromes. In addition, overaccumulation of such structures leads to excessive ROS generation and supply plant's defense-responsive hemoproteins [71]. The importance of these substances in biotic stresses is underlined by the fact that mycotoxins produced by necrotrophic fungi leads to inhibition of porphyrin synthesis [72].

Metabolites from "Phenylpropanoid biosynthesis" and "Flavonoids biosynthesis" pathway are a source for key downstream specialized metabolites involved in antioxidation, photosynthesis and resulting from these properties also plant response to pathogens [73]. Phenylpropanoids in many tissues are presented as soluble form and as bonded components of the cell wall. For studying the second mentioned additional alkaline step of extraction methods not used in our studies should be applied. Therefore only soluble

 doi:10.20944/preprints202207.0378.v1

representatives of metabolome were taken into analysis. Among them different structures as hydroxycinnamic acids, chalcones, flavanes, flavanols, and anthocyanidins which are broadly found in cereals spikes were matched. Conferring ROS scavenging or inhibition of lipid peroxidation is related to 3, 4'-hydroxylation in B ring of core flavonoid skeleton in compilation with unsaturated 2-3 bond and 4-oxo function or galloyl moiety substitution [74]. Therefore catechin, gallocatechin from flavanols, myricetin and quercetin but not kaempferol from flavonols nor flavones might be efficiently involved in ROS scavenge. On the other hand, presence of ferulic, p-coumaric acids, apigenin and luteolin in addition to tyramine derivatives is described in literature as fungal growth inhibitors [75], [76]. Moreover, structures of hydroxycinnamic acids were previously reported as associated to cell wall reinforcement [77] and also as induced upon mycotoxin DON [78]. Multiple role of phenylpropanoids in FHB complement reports of an association with FHB resistance of hydroxycinnamic acid derivatives esterified with amides [77] and quinic acids [79]. Ferulic and caffeic acid are effective inhibitors of *Fusarium* growth, but also act as inhibitors of fungal genes for trichotecenes biosynthesis [80]. Multitasking of hydroxycinnamic acids corroborate our observation about drastic increasing their correlation to other metabolites upon FHB in comparison to control conditions. Among annotated DAMs, ferulic, p-coumaric, caffeic, sinapic and their glycosylated forms were central hubs with the highest number of inter- and intra-connections in correlation network. It cannot be excluded that those metabolites contributed to the kinetics of mycotoxin accumulation observed in our experiments Such complex relationships presumably reflects the multitude of metabolic mechanism driven by those structures.

Triggering of "Ascorbate and aldarate metabolism" as conserved immune response can be related to ascorbic acid accumulation as another effective antioxidant [81] but also regulators of photosynthesis and transmembrane electron transport [82].

Wheat and barley commonly annotated lignan biosynthesis pathway. Such phenylpropanoid monolignols precursors were previously reported as FHB -related in resistant barley [83] and resistant wheat [84]. Pinoresinol and their derivatives were reported as induced during FHB in highly resistant wheat Sumai-3 [85]. Our analysis matched disturbances in pinoresinol and their derivatives in both resistant and susceptible wheat cultivars which can be explain by specificity of developmental stage, differences in resistance type and fusarium strains differences in producing mycotoxin as in mentioned publication, the trichotecenes production highly influence lignan accumulation in host plants. On the other hand, we found secoisolariciresinol and two glycosides of lignan derivative as commonly affected DAMs for resistant genotypes while matairesinol and lyoniresinol glucoside were commonly DAMs for susceptible genotypes. Limiting number of reports suggests in vivo and in vitro lignan inhibiting effect on fusarium mycotoxin production [86] and improving cell wall thickness [73] contributing to increasing plant resistance to pathogen.

Conservative DAMs from pathways related to aromatic amino acids "Tyrosine metabolism" at T1 and "Tryptophan metabolism" can be related after a stepwise of methylation to production of antifungal alkaloids of grasses hordenine ((N,N-dimethyltyramine), serotonin and tryptamine in Poaceae plants [87] . Induction of tyrosine- and tryptophan-derived metabolites by Fusarium was previously observed in Bd [88], barley [83] and wheat [81], [85]. Tyrosine is link to lignin formation via TAL (Tyr ammonia-lyase) enzyme exclusively presented in grasses [89]. On the other hand, hordenine induces plant defense response through the jasmonate-dependent defense pathway [90].

Metabolic pathways related to unsaturated fatty acids were commonly affected both as conservative and genotype-specific factors. FHB-responsive "α-Linolenic acid metabolism" is a source of precursors for jasmonic acid and methyl jasmonate. Those plant hormones are known for enhancing wheat resistance to necrotrophic pathogens [91]. Induction of Ja and JA-associated genes was also reported in wheat and Bd upon fusarium inoculation [92], [93]. Studies on rice showed negative cross-talk between inhibition of GA-mediated growth prior to JA-related plant defense [94]. "Linoleic acid metabolism" enriched at T2 for Bd21 in contrast to jasmonate-related α-linolenic acid is a main source of

Preprints (www.preprints.org) | NOT PEER-REVIEWED | Posted: 26 July 2022 doi:10.20944/preprints202207.0378.v1

H_2O_2 from β-oxidation processes. Both of this unsaturated fatty acid precursors were previously described as related to FHB resistance in barley leaves and antifungal properties for those compounds were reported [95]. Metabolites from "Arachidonic acid metabolism" are known from eliciting general stress signaling networks during FHB [96]. DAMs matched from this pathway in cooperation with lignan biosynthesis are responsible for strong changes in membrane ingredients as well as extracellular barrier based on cutin and suberin [97]. These findings agree with previous metabolomic studies revealing unsaturated fatty acids, in addition to phenylpropanoids and flavonoids as resistance-related to FHB in barley [83].

4.8. Genotype-specific metabolomic response to FHB

Four nitrogens-containing metabolites from "Caffeine metabolism" were matched in Hr as resistance-related. Paraxanthine and theobromine from this pathway can be transformed by xanthine dehydrogenase/oxidase (KEGG id K00106) to 1,7-dimethyluric acid and 3,7-dimethyluric acid, respectively in *A. thaliana.* Mentioned enzyme participates in defense modulation by antioxidants production [98]. Presence of this particular compounds were not confirmed in our analysis by MS/MS spectra, however, shows the direction of further analyzes towards the search for similar four nitrogen-containing structures as FHB-responsive. Matching metabolites related to purine ring from "Caffeine biosynthesis" highlight triggering of nitrogen reservoir during FHB in wheat as was previously observed [99]. Adenosine, guanosine and their phosphorylated forms of IMP, AMP and GMP are critical metabolites for vegetative growth, sexual/asexual reproduction and pathogenesis in *F. graminearum* [100]. In addition, adenine phosphoribosyltransferase has been reported as critical in enhancing oxidative stress tolerance in *A. thaliana* [101]. Some transcripts encoded enzymes from purine metabolism were reported as FHB resistance-related in wheat [102]. What is more, these compounds diversified resistant and susceptible wheat cultivars during FHB [103]. Taken together all these observations with fact that pirimidines and in lesser extension purines were highly correlated to other common DAMs it can be generally assumed that nitrogen metabolism is related to FHB resistance in grasses by multifactorial impacts on the plant-pathogen interactions.

Common metabolites between resistant genotypes of wheat and barley were clearly amino acids. A consistent result was found in previous studies indicating proline and alanine as markers of resistance to FHB in wheat [55]. Our additional databases searching showed proline and proline glucoside in addition to serine and acetylcarnitine as factor not only for wheat but also for barley resistance. In addition, "Arginine and proline metabolism" was enriched in pathway analysis as primarily FHB-triggered in Hr. This pathway is a source of energy as well as nitrate oxide participating in ROS mobilization [104]. The osmolytic features of proline can be used for cellular structures protection [105]. Together with our study, this confirms the potential of being a marker for increasing resistance in Poaceae plants.

Interestingly, sulphur-containing dicarboxylic acids and related to them compounds from "Cysteine and methionine metabolism" were also matched as resistance -conferring in Hr. Those compounds are a source of glutathione and sulphur assimilates. Thiol containing cysteine and glutathione, are crucially important for maintaining and regulating redox homeostasis. Cysteine is the central precursor of all organic molecules containing reduced sulfur such as phytochelatins, proteins, vitamins, cofactors and hormones. In dicots Brassicaceae metabolites from this pathway are precursors of glucosinolates biosynthesis which are involved in immunological reaction to herbivores and pathogens [106].

Contrary, methionine was matched as DAMs shared in susceptible genotypes. Also phenylanine, accumulation was increased during FHB in both susceptible Ts and Hs. This amino acid is known to have higher level in resistant that in susceptible genotype of barley [83]. However, in our experiment the fold change between control and infected plants was significant only in susceptible genotypes, while in resistant the level should be high but constant in term of experimental conditions. Taking into account central role of

 doi:10.20944/preprints202207.0378.v1

phenylalanine in secondary metabolism and its multitasking it role can be profound. The same can be suggested for 12-hydroxyjasmonic acids detected as DAMS common for both susceptible genotypes. 12-Hydroxyjasmonic acid is broadly occurring inactive JA-derived metabolite. Together with it its sulfated and glycosylated forms was considered as switching off element of jasmonate signaling response in barley [107] and other plants [108]. Presence of this metabolite as susceptibility-related can presumably be related to similar impairment of JA-mediated response in Ts and Hs. Contrary, JA and MeJa were annotated as conservative DAMs with high level of correlation with other DAMs suggesting central role for JA-dependent response in FHB, however some inhibition to them processes occurred in susceptible genotypes.

The accumulation of benzoxazinoids correlates with resistance to FHB in wheat and wild barley heads [109]. However, benzoxazinoids biosynthesis is not found in cultivated barley and Bd. Benzoxazinoid accumulation in wheat is regulated by jasmonic acid [110]. Diverse accumulation of different benzoxazinoids was similarly observed by previous analysis tend to search the correlation of FHB resistance to benzoxazinoids accumulation [111]. Equivocal results may be related with the complex biosynthesis and regulatory pathway of beznoxazinoids not fully explore at now.

5. Conclusions

Combining untargeted and targeted approaches allows for stupendous progress in dissection of defense-related metabolites and illustrate their correlation and interaction with other elements of plant immunity. We observed that stability of plant homeostasis during Fc infection is driven by significant metabolome reprogramming. Production of antioxidants and phytoalexins are in ubiquitous interactions with sugar managements and photosynthesis. Plant-pathogen interaction is shaping by plant metabolites with abilities to recognize, inhibit and counteracts pathogenic microbes and their products. The genotype-specific profile of those molecules can boost or hamper the power to combat *F. culmorum*. On the other hand, pathogenic metabolites and sophisticated mechanism of infection determine the plant immunity rendering plant-pathogen interaction quaint. Conserved response elements in all Poaceae plants use common hormone signaling pathways and evolutionary conserved phenylpropanoids, flavonoids, purines and pirimidines in highly correlated network during *F. culmorum* infection. On the other hand, specialized phytoalexins limited in number in resistant genotypes enhanced the inhibition of the pathogenesis in the early stages of infection. We expect that our results concerning conservative and genotype-specific metabolomic elements of immunity will provide information for breeders about metabolomic biomarkers of high resistance to FHB and inhibitions of mycotoxins productions. The pipeline of metabolomic studies with multifactorial experiments followed by DAMs selection and elimination of signals corresponding to mycotoxins can clearly present the picture of pathogen-plant inetraction at metabolome level and may give a baseline to deepen searching of metabolomic marker of enhance resistance to FHB.

Author Contributions: "Conceptualization, A.P. methodology, A.P., A.S.; software, A.P., A.S., M.K ; validation, A.S., J. L-K, investigation, A.P., N.W., A.W., J. K. J. L-K, M. K; writing—original draft preparation, A.P; writing—review and editing, A.S., N.W. J. L-K.; visualization, A.S., M.K, A.P.; supervision, A.P.; project administration, A.P.

Funding: This research was funded by the National Science Centre grant of AP: Sonata 2015/17/D/NZ9/03347.

Informed Consent Statement: All authors have read and agreed to the published version of the manuscript.

Data Availability Statement: Datasets from positive and negative ionization are deposited in a publicly available database Metabolights with accession numbers MTBLS1748 (the URL www.ebi.ac.uk/metabolights/MTBLS1748).

Acknowledgments: We would greatly acknowledge to dr Anetta Kuczyńska,dr Piotr Ogrodowicz and dr Krzysztof Mikołajczak for selection of resistant and susceptible genotypes of barley and seed usage for our experiments. We are also immensely grateful to dr Karolina Krystkowiak for helping to obtain wheat seeds from Breeding Center "Strzelce".

Conflicts of Interest: The authors declare no conflict of interest.

References

1. Oerke, E.C. Crop losses to pests. *The Journal of Agricultural Science* **2006**, *144*, 31-43, doi:10.1017/S0021859605005708.
2. Sutton, J.C. Epidemiology of wheat head blight and maize ear rot caused by Fusarium graminearum. *Canadian Journal of Plant Pathology* **1982**, *4*, 195-209, doi:10.1080/07060668209501326.
3. Tao Y., N.S.W., Huang C., Zhang P., Song S., Sun L., Wu Y. (2016). Brachypodium distachyon is a suitable host plant for study of Barley yellow dwarf virus. Virus Genes 52: 299–302. **Tao Y., Nadege S.W., Huang C., Zhang P., Song S., Sun L., Wu Y. (2016). Brachypodium distachyon is a suitable host plant for study of Barley yellow dwarf virus. Virus Genes 52: 299–302.**
4. Nomura, T.; Ishihara, A.; Imaishi, H.; Ohkawa, H.; Endo, T.R.; Iwamura, H. Rearrangement of the genes for the biosynthesis of benzoxazinones in the evolution of Triticeae species. *Planta* **2003**, *217*, 776-782, doi:10.1007/s00425-003-1040-5.
5. Pasquet, J.C.; Chaouch, S.; Macadré, C.; Balzergue, S.; Huguet, S.; Martin-Magniette, M.L.; Bellvert, F.; Deguercy, X.; Thareau, V.; Heintz, D.; et al. Differential gene expression and metabolomic analyses of Brachypodium distachyon infected by deoxynivalenol producing and non-producing strains of Fusarium graminearum. *BMC Genomics* **2014**, *15*, 629, doi:10.1186/1471-2164-15-629.
6. Kumaraswamy, K.G.; Kushalappa, A.C.; Choo, T.M.; Dion, Y.; Rioux, S. Mass Spectrometry Based Metabolomics to Identify Potential Biomarkers for Resistance in Barley against Fusarium Head Blight (Fusarium graminearum). *Journal of Chemical Ecology* **2011**, *37*, 846-856, doi:10.1007/s10886-011-9989-1.
7. Bollina, V.; Kumaraswamy, G.K.; Kushalappa, A.C.; Choo, T.M.; Dion, Y.; Rioux, S.; Faubert, D.; Hamzehzarghani, H. Mass spectrometry-based metabolomics application to identify quantitative resistance-related metabolites in barley against Fusarium head blight. *Mol Plant Pathol* **2010**, *11*, 769-782, doi:10.1111/j.1364-3703.2010.00643.x.
8. Gunnaiah, R.; Kushalappa, A.C.; Duggavathi, R.; Fox, S.; Somers, D.J. Integrated Metabolo-Proteomic Approach to Decipher the Mechanisms by Which Wheat QTL (Fhb1) Contributes to Resistance against Fusarium graminearum. *PLOS ONE* **2012**, *7*, e40695, doi:10.1371/journal.pone.0040695.
9. Bilska, K.; Stuper-Szablewska, K.; Kulik, T.; Buśko, M.; Załuski, D.; Jurczak, S.; Perkowski, J. Changes in Phenylpropanoid and Trichothecene Production by Fusarium culmorum and F. graminearum Sensu Stricto via Exposure to Flavonoids. *Toxins (Basel)* **2018**, *10*, doi:10.3390/toxins10030110.
10. Skadhauge, B.; Thomsen, K.K.; Von Wettstein, D. The Role of the Barley Testa Layer and its Flavonoid Content in Resistance to Fusarium Infections. *Hereditas* **1997**, *126*, 147-160, doi:https://doi.org/10.1111/j.1601-5223.1997.00147.x.
11. Gardiner, D.M.; Kazan, K.; Praud, S.; Torney, F.J.; Rusu, A.; Manners, J.M. Early activation of wheat polyamine biosynthesis during Fusarium head blight implicates putrescine as an inducer of trichothecene mycotoxin production. *BMC Plant Biol* **2010**, *10*, 289, doi:10.1186/1471-2229-10-289.
12. Peraldi, A.; Beccari, G.; Steed, A.; Nicholson, P. Brachypodium distachyon: a new pathosystem to study Fusarium head blight and other Fusarium diseases of wheat. *BMC Plant Biol* **2011**, *11*, 100, doi:10.1186/1471-2229-11-100.
13. Piasecka, A.; Sawikowska, A.; Krajewski, P.; Kachlicki, P. Combined mass spectrometric and chromatographic methods for in-depth analysis of phenolic secondary metabolites in barley leaves. *J Mass Spectrom* **2015**, *50*, 513-532, doi:10.1002/jms.3557.
14. Ogrodowicz, P.; Kuczyńska, A.; Mikołajczak, K.; Adamski, T.; Surma, M.; Krajewski, P.; Ćwiek-Kupczyńska, H.; Kempa, M.; Rokicki, M.; Jasińska, D. Mapping of quantitative trait loci for traits linked to fusarium head blight in barley. *PLOS ONE* **2020**, *15*, e0222375, doi:10.1371/journal.pone.0222375.
15. Lenc, L.; Czecholiński, G.; Wyczling, D.; Turów, T.; Kaźmierczak, A. Fusarium head blight (FHB) and Fusarium spp. on grain of spring wheat cultivars grown in Poland. *Journal of Plant Protection Research* **2015**, *55*, 266-277, doi:10.1515/jpp-2015-0038.
16. Jiang, G.L.; Shi, J.; Ward, R.W. QTL analysis of resistance to Fusarium head blight in the novel wheat germplasm CJ 9306. I. Resistance to fungal spread. *Theor Appl Genet* **2007**, *116*, 3-13, doi:10.1007/s00122-007-0641-y.
17. Waalwijk, C.; van der Heide, R.; de Vries, I.; van der Lee, T.; Schoen, C.; Costrel-de Corainville, G.; Häuser-Hahn, I.; Kastelein, P.; Köhl, J.; Lonnet, P.; et al. Quantitative Detection of Fusarium Species in Wheat Using TaqMan. *European Journal of Plant Pathology* **2004**, *110*, 481-494, doi:10.1023/B:EJPP.0000032387.52385.13.
18. Golinski, P.; Waskiewicz, A.; Wisniewska, H.; Kiecana, I.; Mielniczuk, E.; Gromadzka, K.; Kostecki, M.; Bocianowski, J.; Rymaniak, E. Reaction of winter wheat (Triticum aestivum L.) cultivars to infection with Fusarium spp.: mycotoxin contamination in grain and chaff. *Food Additives & Contaminants: Part A* **2010**, *27*, 1015-1024, doi:10.1080/19440041003702208.
19. Ożarowski, M.; Piasecka, A.; Gryszczyńska, A.; Sawikowska, A.; Pietrowiak, A.; Opala, B.; Mikołajczak, P.Ł.; Kujawski, R.; Kachlicki, P.; Buchwald, W.; et al. Determination of phenolic compounds and diterpenes in roots of Salvia miltiorrhiza and Salvia przewalskii by two LC–MS tools: Multi-stage and high resolution tandem mass spectrometry with assessment of antioxidant capacity. *Phytochemistry Letters* **2017**, *20*, 331-338, doi:https://doi.org/10.1016/j.phytol.2016.12.001.
20. Piasecka, A.; Sawikowska, A.; Kuczynska, A.; Ogrodowicz, P.; Mikolajczak, K.; Krystkowiak, K.; Gudys, K.; Guzy-Wrobelska, J.; Krajewski, P.; Kachlicki, P. Drought-related secondary metabolites of barley (Hordeum vulgare L.) leaves and their metabolomic quantitative trait loci. *Plant Journal* **2017**, *89*, 898-913, doi:10.1111/tpj.13430.

21. Pluskal, T.; Castillo, S.; Villar-Briones, A.; Oresic, M. MZmine 2: Modular framework for processing, visualizing, and analyzing mass spectrometry-based molecular profile data. *Bmc Bioinformatics* **2010**, *11*, doi:10.1186/1471-2105-11-395.
22. Langfelder, P.; Horvath, S. WGCNA: an R package for weighted correlation network analysis. *BMC Bioinformatics* **2008**, *9*, 559, doi:10.1186/1471-2105-9-559.
23. Shannon, P.; Markiel, A.; Ozier, O.; Baliga, N.S.; Wang, J.T.; Ramage, D.; Amin, N.; Schwikowski, B.; Ideker, T. Cytoscape: a software environment for integrated models of biomolecular interaction networks. *Genome Res* **2003**, *13*, 2498-2504, doi:10.1101/gr.1239303.
24. Pang, Z.; Chong, J.; Zhou, G.; de Lima Morais, D.A.; Chang, L.; Barrette, M.; Gauthier, C.; Jacques, P.-É.; Li, S.; Xia, J. MetaboAnalyst 5.0: narrowing the gap between raw spectra and functional insights. *Nucleic Acids Research* **2021**, *49*, W388-W396, doi:10.1093/nar/gkab382.
25. Kanehisa, M.; Goto, S. KEGG: Kyoto Encyclopedia of Genes and Genomes. *Nucleic Acids Research* **2000**, *28*, 27-30, doi:10.1093/nar/28.1.27.
26. Wishart, D.S.; Tzur, D.; Knox, C.; Eisner, R.; Guo, A.C.; Young, N.; Cheng, D.; Jewell, K.; Arndt, D.; Sawhney, S.; et al. HMDB: the Human Metabolome Database. *Nucleic Acids Res* **2007**, *35*, D521-526, doi:10.1093/nar/gkl923.
27. Sayers, E.W.; Agarwala, R.; Bolton, E.E.; Brister, J R.; Canese, K.; Clark, K.; Connor, R.; Fiorini, N.; Funk, K.; Hefferon, T.; et al. Database resources of the National Center for Biotechnology Information. *Nucleic Acids Research* **2018**, *47*, D23-D28, doi:10.1093/nar/gky1069.
28. Afendi, F.M.; Okada, T.; Yamazaki, M.; Hirai-Morita, A.; Nakamura, Y.; Nakamura, K.; Ikeda, S.; Takahashi, H.; Altaf-Ul-Amin, M.; Darusman, L.K.; et al. KNApSAcK family databases: integrated metabolite-plant species databases for multifaceted plant research. *Plant Cell Physiol* **2012**, *53*, e1, doi:10.1093/pcp/pcr165.
29. Degtyarenko, K.; de Matos, P.; Ennis, M.; Hastings, J.; Zbinden, M.; McNaught, A.; Alcántara, R.; Darsow, M.; Guedj, M.; Ashburner, M. ChEBI: a database and ontology for chemical entities of biological interest. *Nucleic Acids Res* **2008**, *36*, D344-350, doi:10.1093/nar/gkm791.
30. Guijas, C.; Montenegro-Burke, J.R.; Domingo-Almenara, X.; Palermo, A.; Warth, B.; Hermann, G.; Koellensperger, G.; Huan, T.; Uritboonthai, W.; Aisporna, A.E.; et al. METLIN: A Technology Platform for Identifying Knowns and Unknowns. *Anal Chem* **2018**, *90*, 3156-3164, doi:10.1021/acs.analchem.7b04424.
31. Sawada, Y.; Nakabayashi, R.; Yamada, Y.; Suzuki, M.; Sato, M.; Sakata, A.; Akiyama, K.; Sakurai, T.; Matsuda, F.; Aoki, T.; et al. RIKEN tandem mass spectral database (ReSpect) for phytochemicals: A plant-specific MS/MS-based data resource and database. *Phytochemistry* **2012**, *82*, 38-45, doi:https://doi.org/10.1016/j.phytochem.2012.07.007.
32. Wojakowska, A.; Perkowski, J.; Goral, T.; Stobiecki, M. Structural characterization of flavonoid glycosides from leaves of wheat (Triticum aestivum L.) using LC/MS/MS profiling of the target compounds. *Journal of Mass Spectrometry* **2013**, *48*, 329-339, doi:10.1002/jms.3160.
33. Biselli, S.; Hummert, C. Development of a multicomponent method for Fusarium toxins using LC-MS/MS and its application during a survey for the content of T-2 toxin and deoxynivalenol in various feed and food samples. *Food Addit Contam* **2005**, *22*, 752-760, doi:10.1080/02652030500158617.
34. Boddu, J.; Cho, S.; Kruger, W.M.; Muehlbauer, G.J. Transcriptome analysis of the barley-Fusarium graminearum interaction. *Mol Plant Microbe Interact* **2006**, *19*, 407-417, doi:10.1094/mpmi-19-0407.
35. Buerstmayr, H.; Legzdina, L.; Steiner, B.; Lemmens, M. Variation for resistance to Fusarium head blight in spring barley. *Euphytica* **2004**, *137*, 279-290, doi:10.1023/B:EUPH.0000040440.99352.b9.
36. Goddard, R.; Peraldi, A.; Ridout, C.; Nicholson, P. Enhanced Disease Resistance Caused by BRI1 Mutation Is Conserved Between Brachypodium distachyon and Barley (Hordeum vulgare). *Molecular Plant-Microbe Interactions®* **2014**, *27*, 1095-1106, doi:10.1094/mpmi-03-14-0069-r.
37. Tucker, J.R.; Legge, W.G.; Maiti, S.; Hiebert, C.W.; Simsek, S.; Yao, Z.; Xu, W.; Badea, A.; Fernando, W.G.D. Transcriptome Alterations of an in vitro-Selected, Moderately Resistant, Two-Row Malting Barley in Response to 3ADON, 15ADON, and NIV Chemotypes of Fusarium graminearum. *Frontiers in Plant Science* **2021**, *12*, doi:10.3389/fpls.2021.701969.
38. Blümke, A.; Sode, B.; Ellinger, D.; Voigt, C.A. Reduced susceptibility to Fusarium head blight in Brachypodium distachyon through priming with the Fusarium mycotoxin deoxynivalenol. *Mol Plant Pathol* **2015**, *16*, 472-483, doi:10.1111/mpp.12203.
39. Maier, F.J.; Miedaner, T.; Hadeler, B.; Felk, A.; Salomon, S.; Lemmens, M.; Kassner, H.; Schäfer, W. Involvement of trichothecenes in fusarioses of wheat, barley and maize evaluated by gene disruption of the trichodiene synthase (Tri5) gene in three field isolates of different chemotype and virulence. *Mol Plant Pathol* **2006**, *7*, 449-461, doi:10.1111/j.1364-3703.2006.00351.x.
40. Góral, T.; Wiśniewska, H.; Ochodzki, P.; Nielsen, L.K.; Walentyn-Góral, D.; Stępień, Ł. Relationship between Fusarium Head Blight, Kernel Damage, Concentration of Fusarium Biomass, and Fusarium Toxins in Grain of Winter Wheat Inoculated with Fusarium culmorum. *Toxins (Basel)* **2019**, *11*, 2.
41. Hoheneder, F.; Biehl, E.M.; Hofer, K.; Petermeier, J.; Groth, J.; Herz, M.; Rychlik, M.; Heß, M.; Hückelhoven, R. Host Genotype and Weather Effects on Fusarium Head Blight Severity and Mycotoxin Load in Spring Barley. *Toxins (Basel)* **2022**, *14*, 125.
42. Das, K.; Roychoudhury, A. Reactive oxygen species (ROS) and response of antioxidants as ROS-scavengers during environmental stress in plants. *Frontiers in Environmental Science* **2014**, *2*, doi:10.3389/fenvs.2014.00053.
43. Atanasova-Penichon, V.; Barreau, C.; Richard-Forget, F. Antioxidant Secondary Metabolites in Cereals: Potential Involvement in Resistance to Fusarium and Mycotoxin Accumulation. *Frontiers in Microbiology* **2016**, *7*, doi:10.3389/fmicb.2016.00566.
44. Singla, P.; Bhardwaj, R.D.; Kaur, S.; Kaur, J. Antioxidant potential of barley genotypes inoculated with five different pathotypes of Puccinia striiformis f. sp. hordei. *Physiol Mol Biol Plants* **2019**, *25*, 145-157, doi:10.1007/s12298-018-0614-4.

45. Zhou, K.; Hao, J.; Griffey, C.; Chung, H.; O'Keefe, S.F.; Chen, J.; Hogan, S. Antioxidant Properties of Fusarium Head Blight-Resistant and -Susceptible Soft Red Winter Wheat Grains Grown in Virginia. *Journal of Agricultural and Food Chemistry* **2007**, *55*, 3729-3736, doi:10.1021/jf070147a.
46. DESMOND, O.J.; MANNERS, J.M.; STEPHENS, A.E.; MACLEAN, D.J.; SCHENK, P.M.; GARDINER, D.M.; MUNN, A.L.; KAZAN, K. The Fusarium mycotoxin deoxynivalenol elicits hydrogen peroxide production, programmed cell death and defence responses in wheat. *Mol Plant Pathol* **2008**, *9*, 435-445, doi:https://doi.org/10.1111/j.1364-3703.2008.00475.x.
47. Barna, B.; Fodor, J.; Harrach, B.D.; Pogány, M.; Király, Z. The Janus face of reactive oxygen species in resistance and susceptibility of plants to necrotrophic and biotrophic pathogens. *Plant Physiology and Biochemistry* **2012**, *59*, 37-43, doi:https://doi.org/10.1016/j.plaphy.2012.01.014.
48. Castiblanco, V.; Castillo, H.E.; Miedaner, T. Candidate Genes for Aggressiveness in a Natural Fusarium culmorum Population Greatly Differ between Wheat and Rye Head Blight. *J Fungi (Basel)* **2018**, *4*, doi:10.3390/jof4010014.
49. Khaledi, N.; Taheri, P.; Falahati-Rastegar, M. Reactive oxygen species and antioxidant system responses in wheat cultivars during interaction with Fusarium species. *Australasian Plant Pathology* **2016**, *45*, 653-670, doi:10.1007/s13313-016-0455-y.
50. Singla, P.; Bhardwaj, R.D.; Kaur, S.; Kaur, J. Antioxidant potential of barley genotypes inoculated with five different pathotypes of Puccinia striiformis f. sp. hordei. *Physiol Mol Biol Plants* **2019**, *25*, 145-157, doi:10.1007/s12298-018-0614-4.
51. Winkelmüller, T.M.; Entila, F.; Anver, S.; Piasecka, A.; Song, B.; Dahms, E.; Sakakibara, H.; Gan, X.; Kułak, K.; Sawikowska, A.; et al. Gene expression evolution in pattern-triggered immunity within Arabidopsis thaliana and across Brassicaceae species. *Plant Cell* **2021**, *33*, 1863-1887, doi:10.1093/plcell/koab073.
52. Pan, Y.; Liu, Z.; Rocheleau, H.; Fauteux, F.; Wang, Y.; McCartney, C.; Ouellet, T. Transcriptome dynamics associated with resistance and susceptibility against fusarium head blight in four wheat genotypes. *BMC Genomics* **2018**, *19*, 642, doi:10.1186/s12864-018-5012-3.
53. Cuperlovic-Culf, M.; Wang, L.; Forseille, L.; Boyle, K.; Merkley, N.; Burton, I.; Fobert, P.R. Metabolic Biomarker Panels of Response to Fusarium Head Blight Infection in Different Wheat Varieties. *PLOS ONE* **2016**, *11*, e0153642, doi:10.1371/journal.pone.0153642.
54. Surendra, A.; Cuperlovic-Culf, M. Database of resistance related metabolites in Wheat Fusarium head blight Disease (MWFD). *Database* **2017**, *2017*, doi:10.1093/database/bax076.
55. Zhao, P.; Gu, S.; Han, C.; Lu, Y.; Ma, C.; Tian, J.; Bi, J.; Deng, Z.; Wang, Q.; Xu, Q. Targeted and Untargeted Metabolomics Profiling of Wheat Reveals Amino Acids Increase Resistance to Fusarium Head Blight. *Frontiers in Plant Science* **2021**, *12*, doi:10.3389/fpls.2021.762605.
56. Cajka, T.; Vaclavikova, M.; Dzuman, Z.; Vaclavik, L.; Ovesna, J.; Hajslova, J. Rapid LC-MS-based metabolomics method to study the Fusarium infection of barley. *Journal of Separation Science* **2014**, *37*, 912-919, doi:https://doi.org/10.1002/jssc.201301292.
57. Jiang, G.-L.; Shi, J.; Ward, R.W. QTL analysis of resistance to Fusarium head blight in the novel wheat germplasm CJ 9306. I. Resistance to fungal spread. *Theoretical and Applied Genetics* **2007**, *116*, 3-13, doi:10.1007/s00122-007-0641-y.
58. Schöneberg, T.; Musa, T.; Forrer, H.-R.; Mascher, F.; Bucheli, T.D.; Bertossa, M.; Keller, B.; Vogelgsang, S. Infection conditions of Fusarium graminearum in barley are variety specific and different from those in wheat. *European Journal of Plant Pathology* **2018**, *151*, 975-989, doi:10.1007/s10658-018-1434-7.
59. Gauthier, L.; Atanasova-Penichon, V.; Chéreau, S.; Richard-Forget, F. Metabolomics to Decipher the Chemical Defense of Cereals against Fusarium graminearum and Deoxynivalenol Accumulation. *International Journal of Molecular Sciences* **2015**, *16*, 24839-24872.
60. de Vries, S.; Fürst-Jansen, J.M.R.; Irisarri, I.; Dhabalia Ashok, A.; Ischebeck, T.; Feussner, K.; Abreu, I.N.; Petersen, M.; Feussner, I.; de Vries, J. The evolution of the phenylpropanoid pathway entailed pronounced radiations and divergences of enzyme families. *The Plant Journal* **2021**, *107*, 975-1002, doi:https://doi.org/10.1111/tpj.15387.
61. Gangl, R.; Tenhaken, R. Raffinose Family Oligosaccharides Act As Galactose Stores in Seeds and Are Required for Rapid Germination of Arabidopsis in the Dark. *Frontiers in Plant Science* **2016**, *7*, doi:10.3389/fpls.2016.01115.
62. Bolouri-Moghaddam, M.R.; Le Roy, K.; Xiang, L.; Rolland, F.; Van den Ende, W. Sugar signalling and antioxidant network connections in plant cells. *The FEBS Journal* **2010**, *277*, 2022-2037, doi:https://doi.org/10.1111/j.1742-4658.2010.07633.x.
63. Hamzehzarghani, H.; Kushalappa, A.C.; Dion, Y.; Rioux, S.; Comeau, A.; Yaylayan, V.; Marshall, W.D.; Mather, D.E. Metabolic profiling and factor analysis to discriminate quantitative resistance in wheat cultivars against fusarium head blight. *Physiological and Molecular Plant Pathology* **2005**, *66*, 119-133, doi:https://doi.org/10.1016/j.pmpp.2005.05.005.
64. Campos-Bermudez, V.A.; Fauguel, C.M.; Tronconi, M.A.; Casati, P.; Presello, D.A.; Andreo, C.S. Transcriptional and Metabolic Changes Associated to the Infection by Fusarium verticillioides in Maize Inbreds with Contrasting Ear Rot Resistance. *PLOS ONE* **2013**, *8*, e61580, doi:10.1371/journal.pone.0061580.
65. Thorpe, M.R.; MacRae, E.A.; Minchin, P.E.H.; Edwards, C.M. Galactose stimulation of carbon import into roots is confined to the Poaceae. *Journal of Experimental Botany* **1999**, *50*, 1613-1618, doi:10.1093/jxb/50.339.1613.
66. Kanwar, P.; Jha, G. Alterations in plant sugar metabolism: signatory of pathogen attack. *Planta* **2019**, *249*, 305-318, doi:10.1007/s00425-018-3018-3.
67. Skalska, A.; Beckmann, M.; Corke, F.; Savas Tuna, G.; Tuna, M.; Doonan, J.H.; Hasterok, R.; Mur, L.A.J. Metabolomic Variation Aligns with Two Geographically Distinct Subpopulations of Brachypodium Distachyon before and after Drought Stress. *Cells* **2021**, *10*, 683.
68. Guzman, M.I.; Eugene, A.J. Aqueous Photochemistry of 2-Oxocarboxylic Acids: Evidence, Mechanisms, and Atmospheric Impact. *Molecules* **2021**, *26*, 5278.

69. Yang, H.; Luo, P. Changes in Photosynthesis Could Provide Important Insight into the Interaction between Wheat and Fungal Pathogens. *Int J Mol Sci* **2021**, *22*, doi:10.3390/ijms22168865.
70. Spanic, V.; Viljevac Vuletic, M.; Drezner, G.; Zdunic, Z.; Horvat, D. Performance Indices in Wheat Chlorophyll a Fluorescence and Protein Quality Influenced by FHB. *Pathogens* **2017**, *6*, doi:10.3390/pathogens6040059.
71. Espinas, N.A.; Kobayashi, K.; Sato, Y.; Mochizuki, N.; Takahashi, K.; Tanaka, R.; Masuda, T. Allocation of Heme Is Differentially Regulated by Ferrochelatase Isoforms in Arabidopsis Cells. *Frontiers in Plant Science* **2016**, *7*, doi:10.3389/fpls.2016.01326.
72. Duke, S.O.; Dayan, F.E. Modes of Action of Microbially-Produced Phytotoxins. *Toxins (Basel)* **2011**, *3*, 1038-1064.
73. SIRANIDOU, E.; KANG, Z.; BUCHENAUER, H. Studies on Symptom Development, Phenolic Compounds and Morphological Defence Responses in Wheat Cultivars Differing in Resistance to Fusarium Head Blight. *Journal of Phytopathology* **2002**, *150*, 200-208, doi:https://doi.org/10.1046/j.1439-0434.2002.00738.x.
74. Wolfe, K.L.; Liu, R.H. Structure−Activity Relationships of Flavonoids in the Cellular Antioxidant Activity Assay. *Journal of Agricultural and Food Chemistry* **2008**, *56*, 8404-8411, doi:10.1021/jf8013074.
75. Piasecka, A.; Jedrzejczak-Rey, N.; Bednarek, P. Secondary metabolites in plant innate immunity: conserved function of divergent chemicals. *New Phytologist* **2015**, *206*, 948-964, doi:https://doi.org/10.1111/nph.13325.
76. Du, Y.; Chu, H.; Wang, M.; Chu, I.K.; Lo, C. Identification of flavone phytoalexins and a pathogen-inducible flavone synthase II gene (SbFNSII) in sorghum. *Journal of Experimental Botany* **2009**, *61*, 983-994, doi:10.1093/jxb/erp364.
77. Karre, S.; Kumar, A.; Yogendra, K.; Kage, U.; Kushalappa, A.; Charron, J.B. HvWRKY23 regulates flavonoid glycoside and hydroxycinnamic acid amide biosynthetic genes in barley to combat Fusarium head blight. *Plant Mol Biol* **2019**, *100*, 591-605, doi:10.1007/s11103-019-00882-2.
78. Doppler, M.; Kluger, B.; Bueschl, C.; Steiner, B.; Buerstmayr, H.; Lemmens, M.; Krska, R.; Adam, G.; Schuhmacher, R. Stable Isotope-Assisted Plant Metabolomics: Investigation of Phenylalanine-Related Metabolic Response in Wheat Upon Treatment With the Fusarium Virulence Factor Deoxynivalenol. *Frontiers in Plant Science* **2019**, *10*, doi:10.3389/fpls.2019.01137.
79. Chamarthi, S.K.; Kumar, K.; Gunnaiah, R.; Kushalappa, A.C.; Dion, Y.; Choo, T.M. Identification of fusarium head blight resistance related metabolites specific to doubled-haploid lines in barley. *European Journal of Plant Pathology* **2014**, *138*, 67-78, doi:10.1007/s10658-013-0302-8.
80. Boutigny, A.-L.; Barreau, C.; Atanasova-Penichon, V.; Verdal-Bonnin, M.-N.; Pinson-Gadais, L.; Richard-Forget, F. Ferulic acid, an efficient inhibitor of type B trichothecene biosynthesis and Tri gene expression in Fusarium liquid cultures. *Mycological Research* **2009**, *113*, 746-753, doi:https://doi.org/10.1016/j.mycres.2009.02.010.
81. Dhokane, D.; Karre, S.; Kushalappa, A.C.; McCartney, C. Integrated Metabolo-Transcriptomics Reveals Fusarium Head Blight Candidate Resistance Genes in Wheat QTL-Fhb2. *PLoS One* **2016**, *11*, e0155851, doi:10.1371/journal.pone.0155851.
82. Smirnoff, N. Ascorbic acid metabolism and functions: A comparison of plants and mammals. *Free Radic Biol Med* **2018**, *122*, 116-129, doi:10.1016/j.freeradbiomed.2018.03.033.
83. Kumaraswamy, G.K.; Kushalappa, A.C.; Choo, T.M.; Dion, Y.; Rioux, S. Differential metabolic response of barley genotypes, varying in resistance, to trichothecene-producing and -nonproducing (tri5−) isolates of Fusarium graminearum. *Plant Pathology* **2012**, *61*, 509-521, doi:https://doi.org/10.1111/j.1365-3059.2011.02528.x.
84. Lionetti, V.; Giancaspro, A.; Fabri, E.; Giove, S.L.; Reem, N.; Zabotina, O.A.; Blanco, A.; Gadaleta, A.; Bellincampi, D. Cell wall traits as potential resources to improve resistance of durum wheat against Fusarium graminearum. *BMC Plant Biol* **2015**, *15*, 6, doi:10.1186/s12870-014-0369-1.
85. Gunnaiah, R.; Kushalappa, A.C. Metabolomics deciphers the host resistance mechanisms in wheat cultivar Sumai-3, against trichothecene producing and non-producing isolates of Fusarium graminearum. *Plant Physiol Biochem* **2014**, *83*, 40-50, doi:10.1016/j.plaphy.2014.07.002.
86. Kulik, T.; Buśko, M.; Pszczółkowska, A.; Perkowski, J.; Okorski, A. Plant lignans inhibit growth and trichothecene biosynthesis in Fusarium graminearum. *Letters in Applied Microbiology* **2014**, *59*, 99-107, doi:https://doi.org/10.1111/lam.12250.
87. Powell, J.J.; Carere, J.; Sablok, G.; Fitzgerald, T.L.; Stiller, J.; Colgrave, M.L.; Gardiner, D.M.; Manners, J.M.; Vogel, J.P.; Henry, R.J.; et al. Transcriptome analysis of Brachypodium during fungal pathogen infection reveals both shared and distinct defense responses with wheat. *Scientific Reports* **2017**, *7*, 17212, doi:10.1038/s41598-017-17454-3.
88. Pasquet, J.C.; Chaouch, S.; Macadre, C.; Balzergue, S.; Huguet, S.; Martin-Magniette, M.L.; Bellvert, F.; Deguercy, X.; Thareau, V.; Heintz, D.; et al. Differential gene expression and metabolomic analyses of Brachypodium distachyon infected by deoxynivalenol producing and non-producing strains of Fusarium graminearum. *Bmc Genomics* **2014**, *15*, doi:10.1186/1471-2164-15-629.
89. Barros, J.; Serrani-Yarce, J.C.; Chen, F.; Baxter, D.; Venables, B.J.; Dixon, R.A. Role of bifunctional ammonia-lyase in grass cell wall biosynthesis. *Nature Plants* **2016**, *2*, 16050, doi:10.1038/nplants.2016.50.
90. Ishiai, S.; Kondo, H.; Hattori, T.; Mikami, M.; Aoki, Y.; Enoki, S.; Suzuki, S. Hordenine is responsible for plant defense response through jasmonate-dependent defense pathway. *Physiological and Molecular Plant Pathology* **2016**, *96*, 94-100, doi:https://doi.org/10.1016/j.pmpp.2016.10.003.
91. Li, G.; Yen, Y. Jasmonate and Ethylene Signaling Pathway May Mediate Fusarium Head Blight Resistance in Wheat. *Crop Science* **2008**, *48*, 1888-1896, doi:https://doi.org/10.2135/cropsci2008.02.0097.
92. Sun, Y.; Xiao, J.; Jia, X.; Ke, P.; He, L.; Cao, A.; Wang, H.; Wu, Y.; Gao, X.; Wang, X. The role of wheat jasmonic acid and ethylene pathways in response to Fusarium graminearum infection. *Plant Growth Regulation* **2016**, *80*, 69-77, doi:10.1007/s10725-016-0147-1.

93. Kouzai, Y.; Kimura, M.; Yamanaka, Y.; Watanabe, M.; Matsui, H.; Yamamoto, M.; Ichinose, Y.; Toyoda, K.; Onda, Y.; Mochida, K.; et al. Expression profiling of marker genes responsive to the defence-associated phytohormones salicylic acid, jasmonic acid and ethylene in Brachypodium distachyon. *BMC Plant Biol* **2016**, *16*, 59, doi:10.1186/s12870-016-0749-9.
94. Yang, D.-L.; Yao, J.; Mei, C.-S.; Tong, X.-H.; Zeng, L.-J.; Li, Q.; Xiao, L.-T.; Sun, T.-p.; Li, J.; Deng, X.-W.; et al. Plant hormone jasmonate prioritizes defense over growth by interfering with gibberellin signaling cascade. *Proceedings of the National Academy of Sciences* **2012**, *109*, E1192-E1200, doi:10.1073/pnas.1201616109.
95. Walters, D.; Raynor, L.; Mitchell, A.; Walker, R.; Walker, K. Antifungal activities of four fatty acids against plant pathogenic fungi. *Mycopathologia* **2004**, *157*, 87-90, doi:10.1023/b:myco.0000012222.68156.2c.
96. Savchenko, T.; Walley, J.W.; Chehab, E.W.; Xiao, Y.; Kaspi, R.; Pye, M.F.; Mohamed, M.E.; Lazarus, C.M.; Bostock, R.M.; Dehesh, K. Arachidonic acid: an evolutionarily conserved signaling molecule modulates plant stress signaling networks. *Plant Cell* **2010**, *22*, 3193-3205, doi:10.1105/tpc.110.073858.
97. He, M.; Ding, N.-Z. Plant Unsaturated Fatty Acids: Multiple Roles in Stress Response. *Frontiers in plant science* **2020**, *11*, 562785-562785, doi:10.3389/fpls.2020.562785.
98. Ma, X.; Wang, W.; Bittner, F.; Schmidt, N.; Berkey, R.; Zhang, L.; King, H.; Zhang, Y.; Feng, J.; Wen, Y.; et al. Dual and Opposing Roles of Xanthine Dehydrogenase in Defense-Associated Reactive Oxygen Species Metabolism in Arabidopsis. *Plant Cell* **2016**, *28*, 1108-1126, doi:10.1105/tpc.15.00880.
99. Ashihara, H.; Crozier, A. Caffeine: a well known but little mentioned compound in plant science. *Trends in Plant Science* **2001**, *6*, 407-413, doi:https://doi.org/10.1016/S1360-1385(01)02055-6.
100. Sun, M.; Bian, Z.; Luan, Q.; Chen, Y.; Wang, W.; Dong, Y.; Chen, L.; Hao, C.; Xu, J.-R.; Liu, H. Stage-specific regulation of purine metabolism during infectious growth and sexual reproduction in Fusarium graminearum. *New Phytologist* **2021**, *230*, 757-773, doi:https://doi.org/10.1111/nph.17170.
101. Sukrong, S.; Yun, K.-Y.; Stadler, P.; Kumar, C.; Facciuolo, T.; Moffatt, B.A.; Falcone, D.L. Improved Growth and Stress Tolerance in the Arabidopsis oxt1 Mutant Triggered by Altered Adenine Metabolism. *Molecular Plant* **2012**, *5*, 1310-1332, doi:https://doi.org/10.1093/mp/sss065.
102. Li, X.; Zhong, S.; Chen, W.; Fatima, S.A.; Huang, Q.; Li, Q.; Tan, F.; Luo, P. Transcriptome Analysis Identifies a 140 kb Region of Chromosome 3B Containing Genes Specific to Fusarium Head Blight Resistance in Wheat. *International journal of molecular sciences* **2018**, *19*, 852, doi:10.3390/ijms19030852.
103. Sun, Z.; Hu, Y.; Zhou, Y.; Jiang, N.; Hu, S.; Li, L.; Li, T. tRNA-derived fragments from wheat are potentially involved in susceptibility to Fusarium head blight. *BMC Plant Biol* **2022**, *22*, 3, doi:10.1186/s12870-021-03393-9.
104. ZEIER, J. New insights into the regulation of plant immunity by amino acid metabolic pathways. *Plant, Cell & Environment* **2013**, *36*, 2085-2103, doi:https://doi.org/10.1111/pce.12122.
105. Role of Proline in Pathogen and Host Interactions. *Antioxidants & Redox Signaling* **2019**, *30*, 683-709, doi:10.1089/ars.2017.7335.
106. Czerniawski, P.; Piasecka, A.; Bednarek, P. Evolutionary changes in the glucosinolate biosynthetic capacity in species representing Capsella, Camelina and Neslia genera. *Phytochemistry* **2021**, *181*, 112571, doi:https://doi.org/10.1016/j.phytochem.2020.112571.
107. Miersch, O.; Kramell, R.; Parthier, B.; Wasternack, C. Structure–activity relations of substituted, deleted or stereospecifically altered jasmonic acid in gene expression of barley leaves. *Phytochemistry* **1999**, *50*, 353-361, doi:https://doi.org/10.1016/S0031-9422(98)00597-4.
108. Gidda, S.K.; Miersch, O.; Levitin, A.; Schmidt, J.; Wasternack, C.; Varin, L. Biochemical and Molecular Characterization of a Hydroxyjasmonate Sulfotransferase from Arabidopsis thaliana*. *Journal of Biological Chemistry* **2003**, *278*, 17895-17900, doi:https://doi.org/10.1074/jbc.M211943200.
109. Dick, R.; Rattei, T.; Haslbeck, M.; Schwab, W.; Gierl, A.; Frey, M. Comparative Analysis of Benzoxazinoid Biosynthesis in Monocots and Dicots: Independent Recruitment of Stabilization and Activation Functions *Plant Cell* **2012**, *24*, 915-928, doi:10.1105/tpc.112.096461.
110. Sue, M.; Fujii, M.; Fujimaki, T. Increased benzoxazinoid (Bx) levels in wheat seedlings via jasmonic acid treatment and etiolation and their effects on Bx genes including Bx6. *Biochemistry and Biophysics Reports* **2021**, *27*, 101059, doi:https://doi.org/10.1016/j.bbrep.2021.101059.
111. Søltoft, M.; Jørgensen, L.N.; Svensmark, B.; Fomsgaard, I.S. Benzoxazinoid concentrations show correlation with Fusarium Head Blight resistance in Danish wheat varieties. *Biochemical Systematics and Ecology* **2008**, *36*, 245-259, doi:https://doi.org/10.1016/j.bse.2007.10.008.

 doi:10.20944/preprints202207.0378.v1

Supplementary Materials

Figure S1. LC-MS peaks corresponding to mycotoxins from one of representative samples of Hr inoculated by *F. culmorum* at T2 extracted from total ion chromatogram. The *m*/*z* measured values of detected ions were compared to exact mass calculated for chemical formula representing particular ions and the error of *m*/*z* measurement for (A) Ions corresponding to T2 toxin (T2) and diacetoxyscirpenol (DAS) detected at positive ionization; (B) Ions corresponding to zearalenone (ZEN), nivalenol (NIV), and deoxynivalenol (DON) detected at negative ionization.

Preprints (www.preprints.org) | NOT PEER-REVIEWED | Posted: 26 July 2022 doi:10.20944/preprints202207.0378.v1

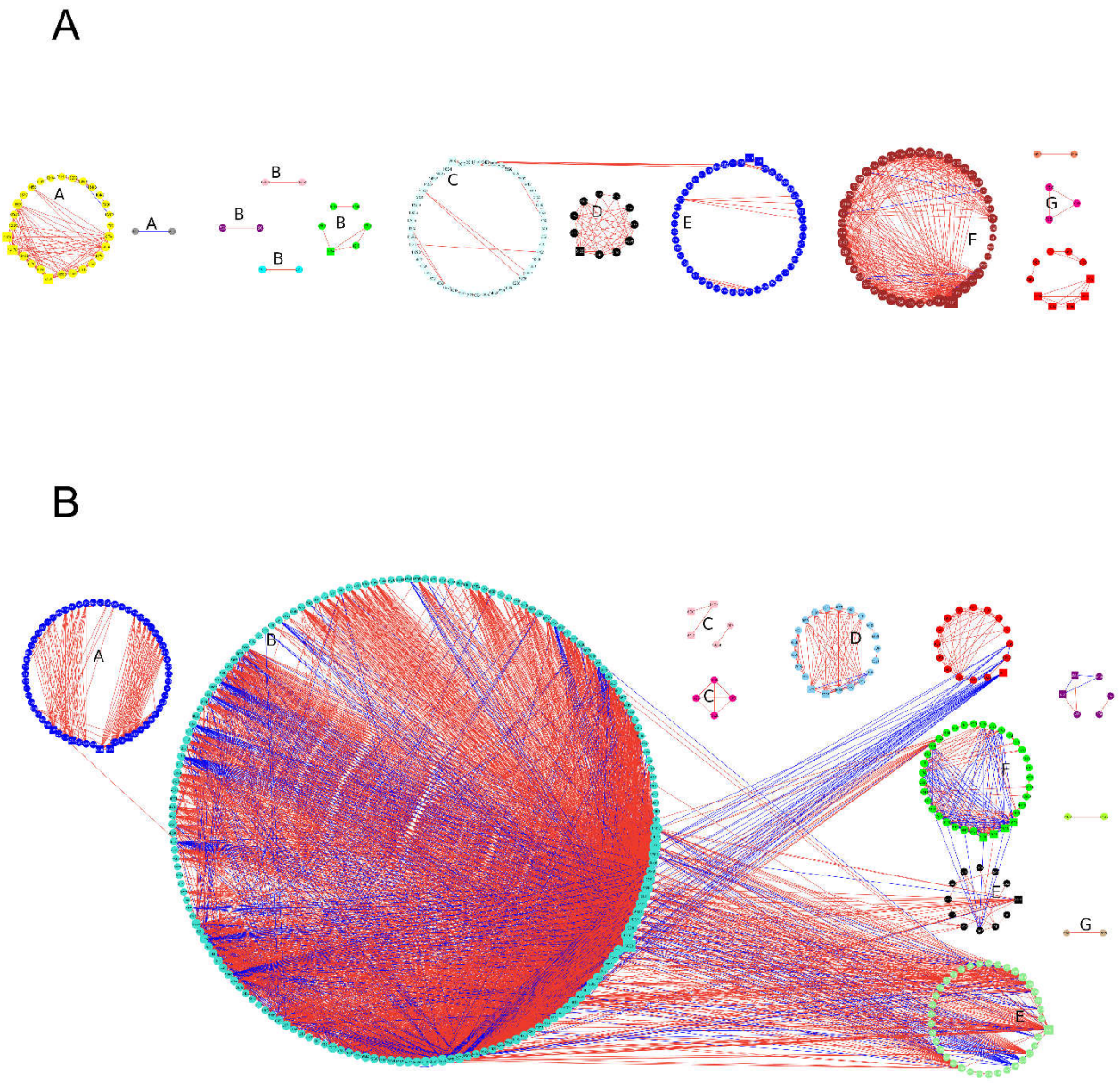

Figure S2. The correlation network of metabolites observed (A) at T1 in control conditions, (B) at T1 after *F. culmorum* inoculation. Metabolites are represented by circles with numbers. The size of the circle is proportional to the number of edges/connections created by this compound. Squares denote hubs, i.e., compounds with the highest number of connections. Edges link highly correlated metabolites. Modules of metabolites are visualized by different colors. Only edges corresponding to elements of the topological overlap matrix greater than 0.25 are shown, both within and between modules, red edges—positive correlations, blue edges—negative correlations. The modules with a large number of metabolites (>60%) occurring in both control and treatment are marked with letters (A)–(G).

Preprints (www.preprints.org) | NOT PEER-REVIEWED | Posted: 26 July 2022 doi:10.20944/preprints202207.0378.v1

Table S1: LC-MS signals corresponding to mycotoxins detected in our experiments which was removed from statistical analysis after processing of raw LC-MS data. Column "Nr org" is number assigned to certain peak in processing of LC-MS data after alignment. Column "Fragmentation" is the most intense typical product ions served for mycotoxins identification. Symbol "Bd" is for *Brachypodium distachyon* Bd21 line, "Hs" is for *Hordeum vulgare* FHB - susceptible genotypes, "Hr" is for *Hordeum vulgare* FHB - resistant genotypes, "Ts" is for *Triticum aestivum* FHB - susceptible cultivar and "Tr" is for *Triticum aestivum* FHB - resistant cultivar.

Table S2. Results of three-way ANOVA conducted on processed LC-MS data combined from positive and negative ionization. Sheet entitled: "peak_list" contains assigned number of peaks in aligned data table with retention time and m/z valued for detected peaks. Sheet entitled: "Means" contains mean values for aligned peaks for all biological repetitions taken for ANOVA, sheet entitled: "Sem" contains standard deviation for corresponding means values, sheet entitled: "P-values_Fdr_Tests_Dams" contains the q-values (FDR) for all factors and their interactions, the fold change calculation and DAMs selection. In sheets "Means" and "Sem" symbol "Bd" is for *Brachypodium distachyon* Bd21 line, "Hs" is for *Hordeum vulgare* FHB - susceptible genotypes, "Hr" is for *Hordeum vulgare* FHB - resistant genotypes, "Ts" is for *Triticum aestivum* FHB - susceptible cultivar and "Tr" is for *Triticum aestivum* FHB - resistant cultivar; number "1" before genotype symbol is for control and number "2" before genotype symbol is for plants with *F. culmorum.*

Table S3. Entire results of functional pathway enrichment on the basis of all signals annotated by MetaboAnalyst 5 at T1 and T2 time points unique for particular genotype and common for all genotypes. Sheet entitled: "pathway enrichment" contains the metabolic pathways matched at KEGG database. Hits is a number of matched compounds from our analysis, FDR (false discovery rate) is a post-hoc controlling procedure, Impact is a pathway impact value related to number of links occurred upon a node in pathway topology graph. Sheet entitled: "annotation" contains the KEGG identificator of annotated metabolites and also corresponding identificator in HMDB, PubChem databaes as well as SMILES code for metabolite. Symbol "Bd" is for *Brachypodium distachyon* Bd21 line, "Hs" is for *Hordeum vulgare* FHB - susceptible genotypes, "Hr" is for *Hordeum vulgare* FHB - resistant genotypes, "Ts" is for *Triticum aestivum* FHB - susceptible cultivar and "Tr" is for *Triticum aestivum* FHB - resistant cultivar;

Table S4. Entire results of structural enrichment on the basis of all signals annotated by MetaboAnalyst 5 at T1 and T2 time points unique for particular genotype and common for all genotypes. Hits is a number of matched compounds from our analysis in particular structural class, FDR (false discovery rate) is a post-hoc controlling procedure of significance of proper signal matching. Symbol "Bd" is for *Brachypodium distachyon* Bd21 line, "Hs" is for *Hordeum*

 doi:10.20944/preprints202207.0378.v1

vulgare FHB - susceptible genotypes, "Hr" is for *Hordeum vulgare* FHB - resistant genotypes, "Ts" is for *Triticum aestivum* FHB - susceptible cultivar and "Tr" is for *Triticum aestivum* FHB - resistant cultivar;

Table S5. Characterization of expression and normalized expression level for *Tri5, Tri6* and *Zea2* genes related to mycotoxins production by *F. culmorum* strain used in our experiment. Table contains all calculation of p-value from t-test , means values from biological repetitions , standard deviation for means and a graph visualizing the obtained data.

Supplementary method 1. Measurement of *in vitro* expression of genes related to biosynthesis of mycotoxins of *F. culmorum* culture used for inoculation.